ASTRONOMY & ASTROPHYSICS
SUPPLEMENT SERIES

Astron. Astrophys. Suppl. Ser. **116,** 257-287 (1996)

Long- and short-term variability in O-star winds⋆. I. Time series of UV spectra for 10 bright O stars

L. Kaper[1,2,⋆⋆] H.F. Henrichs[1,2], J.S. Nichols[3,⋆⋆⋆], L.C. Snoek[1], H. Volten[1] and G.A.A. Zwarthoed[1]

[1] Astronomical Institute "Anton Pannekoek", University of Amsterdam, Kruislaan 403, 1098 SJ Amsterdam, The Netherlands
[2] Center for High Energy Astrophysics (CHEAF), Kruislaan 403 1098 SJ Amsterdam, The Netherlands
[3] Science Programs, Computer Sciences Corporation, 10000-A Aerospace Road, Lanham-Seabrook, MD 20706, U.S.A.

Received May 18; accepted September 27, 1995

Abstract. — An atlas of time series of ultraviolet spectra is presented for 10 bright O stars. The spectra were obtained with the *International Ultraviolet Explorer* during seven observing campaigns lasting several days over a period of 6 years. The UV P Cygni lines in 9 out of the 10 studied stars exhibit a characteristic pattern of variability in the form of discrete absorption components (DACs) migrating through the absorption troughs on a timescale of a day to a week. This pattern is significantly different for each star, but remains relatively constant during the time span of our observations for a given star. A quantitative evaluation of the statistical significance of the variability is given. The winds of a number of stars appear to vary over the full range of wind velocities: from 0 km s^{-1} up to velocities exceeding the terminal velocity v_∞ of the wind as measured by the asymptotic velocity reached by DACs. The amplitude of variability reaches a maximum at about 0.75 v_∞ in the unsaturated resonance lines of stars showing DACs. In saturated resonance lines we find distinct changes in the steep blue edge. This edge variability is also found, although with smaller amplitude, in unsaturated resonance lines. The subordinate line of N IV at 1718 Å in ξ Per shows weak absorption enhancements at low velocities in the blue-shifted absorption that are clearly associated with the DACs in the UV resonance lines. We interpret these three manifestations of variation as reflecting a single phenomenon. The DACs are the most conspicuous form of the variability. The changes at the edge can often be interpreted as DACs, but superposed on a saturated underlying wind profile; in many cases, however, at the same time two or more absorption events in different stages of their evolution can be identified in the unsaturated profiles, hampering a detailed interpretation of the edge variability. The low velocity absorption enhancements in the subordinate lines are the precursors of DACs when they are formed close to the star. The constancy of the pattern of variability over the years and the (quasi-)periodic recurrence of DACs strongly suggest that rotation of the star is an essential ingredient for controlling wind variability. The observation of low-velocity variations in subordinate lines, which are supposedly formed at the base of the stellar wind, indicate an origin of wind variability close to or at the photosphere of the star.[†]

Key words: stars: early type — stars: mass loss — ultraviolet: stars

1. Introduction

The origin of the observed wind variability on timescales of hours, days, and years, in early-type stars is not yet known. Typical expected timescales for the wind flow, stellar rotation and pulsation in these stars are all in the range of a day to a week, which makes it difficult to disentangle their individual contributions. To make progress it is therefore imperative to study a representative sample of stars, over many timescales and in many wavelength regions. This paper describes the first part of such a comprehensive study.

The *International Ultraviolet Explorer* (IUE) has proved to be a powerful tool for the study of variability

Send offprint requests to: L. Kaper

⋆Based on observations by the International Ultraviolet Explorer, collected at NASA Goddard Space Flight Center and Villafranca Satellite Tracking Station of the European Space Agency

⋆⋆*Present address:* European Southern Observatory, Karl Schwarzschild Str. 2, D-85748 Garching bei München, Germany

⋆⋆⋆Staff member, NASA IUE Observatory, Goddard Space Flight Center, Greenbelt, MD, U.S.A.

†Tables listing the Log of Observations described in this paper are only available in electronic form at the CDS via anonymous ftp 130.79.128.5.

Table 1. Program stars with stellar parameters; Notes: (a) Bright Star Catalogue 1982; (b) Walborn 1972, except HD 210839 Walborn 1973; (c) obtained from Howarth & Prinja (1989); (d) predicted from the empirical relation between $\dot{M}$, L and $T_{\rm eff}$ by Lamers & Leitherer (1993); (e) Prinja et al. (1990), but corrected for the radial velocity; (f) Conti & Ebbets 1977; (g) Gies & Bolton 1986; (h) Gies 1987 and Blaauw 1992

HD	Name	$V^{\rm a}$ (mag.)	Spectral Type[b]	$R_\star^{\rm c}$ ($R_\odot$)	$T_{\rm eff}^{\rm c}$ (K)	$\log L_\star{}^{\rm c}$ ($L_\odot$)	$\dot{M}^{\rm d}$ ($M_\odot$/yr)	$v_\infty{}^{\rm e}$ (km/s)	$v \sin i^{\rm f}$ (km/s)	$v_{\rm rad}^{\rm g}$ (km/s)	Remarks[h]
24912	ξ Per	4.04	O7.5 III(n)((f))	11	36 000	5.3	$3\ 10^{-7}$	2390	200	60	Runaway
30614	α Cam	4.29	O9.5 Ia	22	29 900	5.5	$9\ 10^{-7}$	1600	85	11	Runaway
34656		6.79	O7 II(f)	10	36 800	5.2	$2\ 10^{-7}$	2145	106	−9	Aur OB1
36861	λ Ori A	3.66	O8 III((f))	12	35 000	5.3	$3\ 10^{-7}$	2160	53	33	Ori OB1
37742	ζ Ori A	1.75	O9.7 Ib	29	30 000	5.8	$3\ 10^{-6}$	1885	110	23	Ori OB1
47839	15 Mon	4.66	O7 V((f))	10	41 000	5.4	$4\ 10^{-7}$	2080	63	24	Mon OB1
203064	68 Cyg	5.00	O7.5 III:n((f))	14	36 000	5.5	$7\ 10^{-7}$	2350	274	8	Runaway
209975	19 Cep	5.11	O9.5 Ib	18	30 200	5.4	$6\ 10^{-7}$	1995	75	−15	Cep OB2
210839	λ Cep	5.04	O6 I(n)fp	17	42 000	5.9	$3\ 10^{-6}$	2225	214	−75	Runaway
214680	10 Lac	4.88	O9 V	9	38 000	5.1	$1\ 10^{-7}$	1110	32	−9	Lac OB1

of the supersonically expanding winds of early-type stars. In particular, the blue-shifted absorption part of the P Cygni-shaped profiles of strong ultraviolet resonance lines such as Si IV, C IV, and N V shows dramatic changes with time. Some of these profiles contain "narrow" absorption components, first recognized in *Copernicus* spectra of OB-type stars, at velocities close to the terminal velocity, v_∞, of the wind (e.g. Underhill 1975; Morton 1976; Snow & Morton 1976). Lamers et al. (LGS, 1982) reported the presence of narrow components in 17 out of 26 OB stars at a typical blue-shifted velocity of 0.75 v_∞ and a mean width of about 0.18 v_∞. Later time-resolved studies with the IUE Observatory (e.g. Henrichs 1984; Prinja & Howarth (PH) 1986; Henrichs 1988) showed that these narrow components are variable in velocity and profile. The P Cygni profiles also change at lower outflow velocities, but over a wider velocity range. These absorption enhancements were initially differentiated from the narrow absorption components and called "broad" components. Continuous time series of ultraviolet spectra (cf. Prinja et al. 1987; Prinja & Howarth 1988) revealed that these broad components gradually evolve into narrow components on a timescale of a few days, resulting in the currently accepted nomenclature *discrete absorption components* (DACs).

In many cases DACs can be readily identified in single observations, which allowed Howarth & Prinja (HP, 1989) to detect DACs in more than 80% of a sample containing 203 O stars, essentially all O stars which are accessible with the IUE spectrograph in high dispersion mode. This underlined the ubiquity of DACs and established that variability is a very fundamental characteristic of O-star winds. However, in spite of the near universality of wind variability, the origin of the variability has proved elusive due to the large amount of multi-wavelength, time-resolved data needed. There are only a very few O stars for which detailed time series of DACs have previously been recorded, for obvious logistical reasons. The available case studies clearly showed that monitoring of these stars on an appropriate timescale, which is different for each star, is necessary (see e.g. Henrichs 1988 and Henrichs 1991 for reviews). Because our current progress in understanding the cause of this variability is clearly data limited, we have made a systematic effort to construct the best possible datasets for 10 critically selected O stars. This international project was begun in 1986, with typically 3 to 6 days per year of nearly continuous observations with the IUE satellite. We report here on seven such campaigns over a period of 6 years, resulting in 637 high-resolution spectra. Such an extensive homogeneous dataset is unique, and enabled us to follow both the short time (days) behavior, and long-term trends (years). Almost all these campaigns were simultaneously covered with ground-based spectroscopy of high-resolution and high signal-to-noise ratio, photometry, and polarimetry, using 1− 2.2 m class telescopes. In this paper we present the first of two parts describing the ultraviolet spectroscopic results. The optical data will be presented separately. A number of significant results from these coordinated campaigns have been summarized by Henrichs (1991) and Kaper et al. (1995a).

In the first part (this paper) we present the data of the 10 stars in the form of a time series atlas of ultraviolet spectra for essentially all the variable spectral lines in the short-wavelength range of the IUE camera (1200−2000 Å). A detailed investigation of the statistical significance of the detected variations is presented for each star and each spectral line considered, along with the line profiles. We summarize the main characteristics of the program stars, and describe the main results of the variability study. In the second part (Kaper et al. 1995b, Paper II) we present a procedure to disentangle the variable part of the

profile from the underlying P Cygni profile, which provides a reference template for each star. This enables a detailed quantitative modeling of quotient spectra and a determination of individual DAC properties, such as central velocity, column density and recurrence timescale. A complete description of the analysis and interpretation of these results can be found in Kaper (1993).

In the next section we describe the target list and the reduction method of the observations, followed by a statistical description of the signal-to-noise ratio of IUE spectra of the program stars. In Sect. 4 we collect the observational history of the individual stars, ordered by HD number, and summarize the main results from the atlas. Information on individual spectra can be found in the Appendix[1]. In Sect. 5 we discuss the variability in the form of DACs and in the blue edge. In the last section we summarize our conclusions.

2. Observations

2.1. *The Target list*

We applied the following criteria to select the O stars for our program:

1. The sample stars were chosen to be spectroscopically single stars, or in the case of the presence of a nearby detached visual binary companion, the secondary had negligible flux. This selection was to avoid tidal interaction on the photosphere of the sample star. The multiplicity of O stars is discussed by Garmany et al. (1980), Gies & Bolton (1986) and Musaev & Snezhko (1988).
2. In order to achieve the necessary time resolution, the sample stars were required to have exposure times of less than 15 min to obtain optimally exposed high resolution IUE spectra with a signal-to-noise ratio of approximately 25 and optical spectra with a signal-to-noise ratio of approximately 200 with the available instruments.
3. Only Northern hemisphere objects were selected to insure sufficient coverage from the various ground-based observatories.

The requirement of coordinated space- and ground-based observations during 24 hours per day implied a choice to be made between the Northern and Southern hemisphere. For logistical reasons we have chosen the Northern Hemisphere, because we needed at least three large observatories with the proper instrumentation, approximately equally separated in longitude around the globe. Japan, North America, and Europe were the most easily accessible locations with the proper facilities during the majority of the campaigns.

[1]Tables listing the Log of Observations described in this paper are only available in electronic form at the CDS via anonymous ftp 130.79.128.5.

In Table 1 we list the program stars which fulfilled the above selection criteria, along with the adopted stellar parameters and some of their kinematical properties. The sample comprises 2 main sequence stars, 3 giants, and 5 supergiants, ranging from spectral type O6 to O9.7; all spectral types are taken from Walborn (1972, 1973). There is an unavoidable bias towards supergiants in our magnitude-limited sample.

The listed terminal velocities are corrected for the radial velocities of the stars. We note that 40% of our stars do not belong to a cluster or association, and are considered to be runaway stars (Gies 1987; Blaauw 1992), whereas this fraction is about 20% for the total number of O stars (Blaauw 1992). This might be caused by small-number statistics (Conti, priv. comm.). Runaway stars tend to have higher $v \sin i$ values and a higher helium abundance in their atmosphere, as compared to cluster stars. If a runaway was originally a member of a binary system in which the companion underwent a supernova explosion resulting in a kick-velocity to the system, this would imply that runaway stars are evolved objects which have gained mass from their previous companion (Blaauw 1992). This difference in evolutionary history might perhaps cause other effects in the atmosphere and winds of these stars, but we did not consider this aspect in the current study.

2.2. *Observing campaigns*

The nature of our program required continuous coverage of 24 hours during several days, which was only possible by successfully applying for both NASA and ESA/SERC IUE time. In Table 2 we list the targets observed with IUE in each campaign and the number of high-resolution SWP spectra obtained for each star. In spite of tremendous effort on the part of the staff at both IUE Observatories to schedule uninterupted blocks of observing time for this program, a few gaps in the coverage exist in most of the campaigns of 4−8 hours due to the need to integrate scheduling of longer time resolved monitoring campaigns by other observers or technical difficulties.

The exposure times for ultraviolet spectra depend on the interstellar reddening, and were initially estimated from fluxes measured by previous satellites (ANS, S59) and later adjusted to obtain optimum exposure. It is known that temperature conditions on the IUE spacecraft are directly related to the distortion of the image and ultimately to the resulting signal-to-noise ratio of the data. The parameter used to monitor temperature conditions on the spacecraft, THDA, was evaluated constantly in real-time during the acquisition of the observations for these campaigns. The onboard deck heaters were used whenever necessary to keep the THDA value within a few degrees of the optimal value. All exposures were taken in the large aperture. As a result of these efforts the datasets acquired are of particularly high quality and homogeneous.

Table 2. The number of high-resolution IUE spectra obtained during seven observing campaigns from 1986 to 1992. The total number of spectra is 637. The 7 spectra of ξ Per in February 1991 are not shown, but are similar to spectra obtained during other campaigns. In the last column we list the average exposure time per high-resolution SWP image (the total spacecraft time needed for one image is about 45 min)

Star	Aug. 86	Sep. 87	Oct. 88	Oct. 89	Feb. 91	Oct. 91	Nov. 92	Total	$t_{\rm exp}$
ξ Per	-	33	25	23	7	36	-	124	1m10s
α Cam	-	-	-	-	31	-	-	31	1m50s
HD 34656	-	-	-	-	29	-	-	29	15m00s
λ Ori A	-	-	-	-	-	-	27	27	0m20s
ζ Ori A	-	-	-	-	-	-	26	26	0m05s
15 Mon	-	-	-	-	20	-	-	20	0m43s
68 Cyg	33	29	24	23	-	40	-	149	2m20s
19 Cep	29	11	12	-	-	14	16	82	5m30s
λ Cep	14	10	12	23	24	40	-	123	10m00s
10 Lac	-	-	-	-	-	-	26	26	1m00s

The sampling times during the observing runs were chosen differently for each star and adjusted when necessary, in order to avoid under- or oversampling (especially for the slow rotators). The most appropriate sampling time was determined from earlier exposures, if available, otherwise from estimates based on similarity in spectral type, class, wind-flow timescale and rotation rate.

Simultaneous optical observations from different sites spread over the Northern hemisphere were arranged during five of the campaigns, resulting in 24 hours optical coverage. During each campaign, stars with about equal $v \sin i$ values were chosen. During the campaign from 5 to 8 September 1987 we had optical coverage for 68 Cyg (for preliminary results, see Fullerton et al. 1991b). For the other campaigns, 17 to 19 October 1989, 1 to 5 February 1991, 22 to 26 October 1991, and 7 to 12 November 1992, we collected simultaneous optical observations for all IUE targets. In addition to short time scale variability which could be studied for each star in each individual campaign, long (yearly) timescale variability could be studied for ξ Per, 68 Cyg, 19 Cep (included in 5 campaigns), and λ Cep (included in 6 campaigns).

2.3. *Spectral reduction*

Spectrum extraction was performed using the IUEDR (Starlink) software package written by Giddings (1983a, 1983b). The program starts with the photometrically corrected image; a cross-dispersion scan is made to locate an echelle order and to determine the geometric shift of the echelle spectrum. The individual echelle orders are sequentially extracted using the IUEDR centroid tracking algorithm to center accurately the "extraction slit" on each order. The extraction is performed by area integration, using a sampling rate equivalent to one sample per diagonal pixel along the direction of dispersion (i.e. a rate of $\sqrt{2}$ pixel). All pixels flagged as affected by saturation, fiducial marks, ITF truncation, or otherwise identified as faulty are rejected at this stage.

The wavelength-scale calibration is improved by measuring the central wavelength of three selected interstellar lines (S II 1253.812 Å, Si II 1304.372 Å, C I 1560.310 Å) and computing the mean deviation $\triangle\lambda$ of these lines with respect to their laboratory wavelength; a mean wavelength shift of the form $m\triangle\lambda =$ constant is applied to the spectrum, where m is the echelle order number. The obtained accuracy is better than the instrumental resolution of about 0.1 Å, which is equal to our sampling width.

Shortward of about 1400 Å the echelle orders are very closely spaced and overlap. This may lead to an overestimation of the interorder background level. A first-order correction to the cross-dispersion order overlap problem is made using the algorithm of Bianchi & Bohlin (1984) and a standard value (for early-type stars) of 0.15 is used for the parameter HALC (halation correction). This algorithm does not give perfect results, as can be seen in regions of saturation, which sometimes have negative fluxes.

Echelle ripple correction is performed by optimizing the echelle ripple correction parameter k using Barker's method (1984). This procedure causes the spectra of the different orders to join and overlap properly. The individual echelle orders are combined by mapping them on an evenly spaced wavelength grid, using weights inversely proportional to the optimized ripple correction factors in regions of order overlap. Reseau marks are removed from the spectrum by linear interpolation. The spectra were smoothed using a three-point running mean. Because there exists no reliable absolute flux calibration for IUE high-resolution spectra, the flux level is given in arbitrary units of flux numbers per second (FN/s). Finally, for a given star, the fluxes of all spectra were multiplied by a number (between 0.9 and 1.1) such that the continua outside the well-known variable lines coincide.

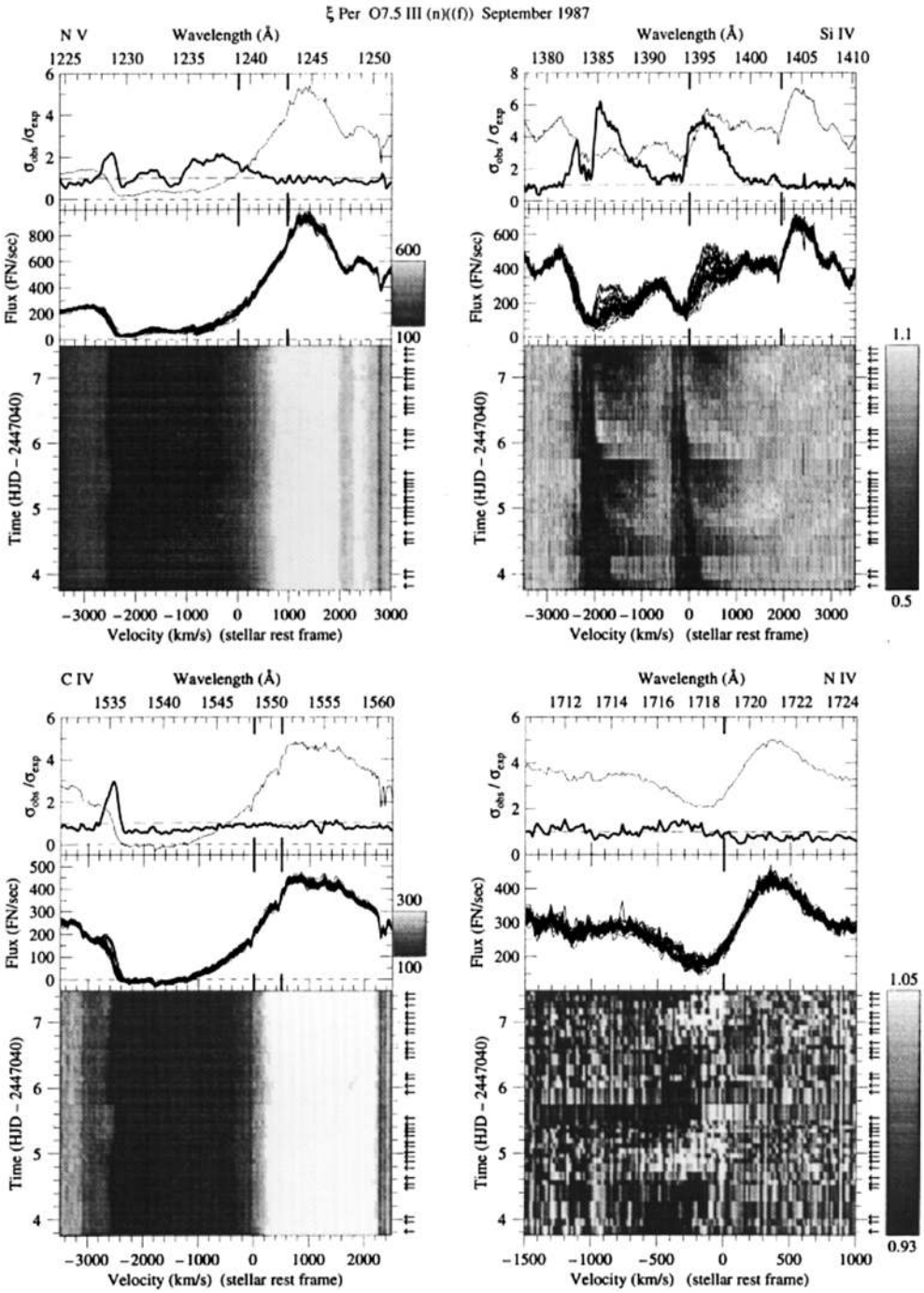

Fig. 1. N v, Si iv, and C iv resonance lines and subordinate N iv line of the O7.5 III(n)((f)) star ξ Per in September 1987. The grey-scale pictures consist of 33 high-resolution IUE spectra with time running upwards (for Si iv and N iv the displayed spectra were divided by a reference spectrum (see text) to optimize the visibility of the variations). The minimum (black) and maximum (white) cuts in flux are given at the side bar that represents the grey-scale conversion. The mid-exposure epochs are indicated by arrows. The individual spectra are overplotted in the middle panel. In the upper panel the variations in the spectra are quantified by the σ-ratio (thick line, see text). The thin line depicts the average spectrum, or, in case of quotient spectra, the reference spectrum. Note the strong variations in the form of DACs in the Si iv doublet and the edge variability in the saturated N v and C iv lines. Also the subordinate N iv line shows variations, but only at low velocities

3. Statistical significance of variability in IUE spectra

The statistical significance of the variability has been determined for each extracted flux point in the spectral regions of interest for the 10 stars in the sample. The technique compares the standard deviation of each point in the spectrum expected, based on the noise characteristics of the instumentation, with the actual observed deviation. The formulation of this statistical significance is described fully in Henrichs et al. (1994a), based on a method developed by Fullerton (1990). A good approximation of the ratio of the observed flux to the expected standard deviation is found to be of the form

$$\frac{F_\lambda}{\sigma_{\rm exp}} = A \tanh \frac{F_\lambda}{B}, \qquad (1)$$

where A corresponds to the maximum S/N for the highest fluxes, and B is a scaling factor. These parameters are determined for each star with a χ^2 fit to more than 4000 points in the average spectrum, excluding the regions containing resonance lines or order overlaps. The values obtained for the 10 datasets are collected in Table 3. In all cases the accuracy in the parameters is better than 2%.

Table 3. Best fit parameters for the noise description of IUE spectra. The flux dependence of $\sigma_{\rm exp}$ was parameterized using a function of the form $F_\lambda/\sigma_{\rm exp} = A \tanh(F_\lambda/B)$, which is obtained using a χ^2 fit. The accuracy of the fitted parameters is better than 2%

Star	A	B
ξ Per	29.6	321
α Cam	28.4	162
HD 34656	29.8	24
λ Ori	28.0	921
ζ Ori	29.0	3959
15 Mon	28.9	554
68 Cyg	29.3	150
19 Cep	28.8	69
λ Cep	34.5	39
10 Lac	30.3	334

The deviation of each actual observed point is measured with respect to the averaged spectrum for each star, which includes all spectra from a given observing campaign. The ratio $\sigma_{\rm obs}/\sigma_{\rm exp}$ should be unity if no significant variations are detectable at the resolution of the instrument.

We point out that the empirical noise model recently presented by Howarth & Smith (1995) which is applied to the same 68 Cyg dataset as in the present paper, gives a more detailed description of the statistical sensitivity by taking the wavelength dependence into account. We have compared their reduced-χ^2 spectra with the σ-ratio for each wavelength bin provided by our method and conclude that in the case of 68 Cyg the two methods give consistent results. We noticed a significant difference only in the saturated trough of the C IV resonance line of 68 Cyg: there they find evidence for variability at velocities down to 0 km s^{-1} which is not indicated by our method. Therefore, we do not expect that the results given in the present paper would be significantly modified when the method developed by Howarth & Smith would have been applied, except perhaps in the low flux regions.

4. Notes on individual stars

Earlier systematic studies on the variable nature of individual O stars can be found in PH, Henrichs et al. (HKZ, 1988), HP, and Fullerton (1990). Below we highlight the observational history of our program stars and describe the observed variability in ultraviolet spectra. The morphology of the variations is clearly demonstrated by showing the time series of the observed spectra in a form where flux is converted into levels of grey. For each star we present the data of the N V (laboratory wavelengths at 1238.821 and 1242.804 Å), Si IV (1393.755 and 1402.770 Å), and C IV (1548.185 and 1550.774 Å) resonance doublets, for each year of observation in separate figures. For ξ Per we also show the N IV subordinate line at 1718.551 Å.

Quotient spectra (indicated by a side bar next to the grey-scale image), rather than the spectra themselves, are used in the grey-scale part of the figure in cases when the visibility of the variations could be improved. In these figures the reference spectrum (a synthetic least-absorption spectrum) used for this purpose is displayed in the upper panel. For the construction of this reference spectrum we refer to Paper II (see also, Kaper 1993).

The y-axis of the time series figures is in units of days, calculated as the heliocentric Julian Date of the observation minus an offset Julian Date in next lower tens of days for each time series. The offset Julian Date for each time series is recorded on the relevant figure and in the associated table in the Appendix. We use the term "Days" to refer to this differential Julian Date for each time series. Arrows to the right of each figure indicate the time of each observation, with the grey scale representation of each spectrum expanded vertically to fill the time between successive observations. We caution the reader to be aware of regions where the gap between successive observations is relatively large and an individual spectrum has been expanded to fill a disproportionately large vertical space in a figure.

The observing dates, exposure times, and other information on the presented spectra in the figures are listed in the Appendix (the numbering of the tables corresponds to the numbering of the figures). In some cases we left out a low-quality spectrum in the grey-scale representation for cosmetic reasons. In the upper panels of the time series

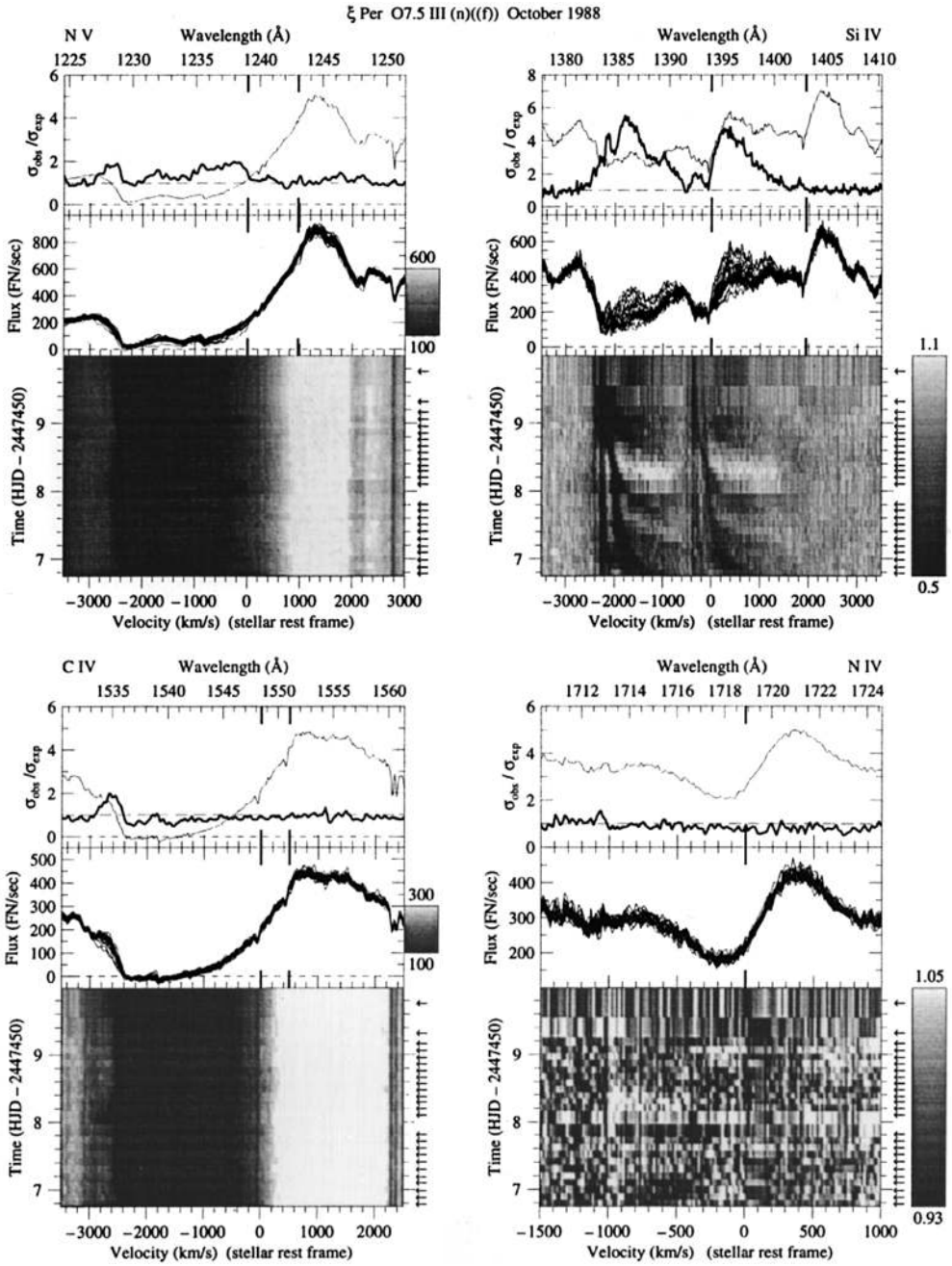

Fig. 2. As in Fig. 1: ξ Per October 1988, 25 spectra. At Day 8.1 a newly formed DAC "crosses" a previous one at a velocity of -1900 km s^{-1} in the Si IV resonance doublet. The new DAC further accelerates to a velocity of -2200 km s^{-1}, while the old one seems to have reached its final velocity. The saturated N V and C IV lines show simultaneous variability in the blue edge. The N IV line does not manifest significant variability, in contrast with e.g. the time series in Fig. 4. Its correlation with the DAC behavior is not obvious from the present time series

the amplitude of variability is quantified using the σ-ratio (thick line), as described in the previous section.

4.1. *HD 24912 (ξ Per) O7.5 III(n)((f))*

ξ Per is a well-known runaway star, which probably originates from the nearby parent Per OB2 association (distance about 350 pc.). Its runaway nature follows mainly from the relative radial velocity of 36 km s^{-1} with respect to the remaining stars of Per OB2 (Blaauw 1992). Garmany et al. (1980), Gies & Bolton (1986), and Jarad et al. (1989) have reported small-amplitude radial velocity variations, but no convincing periodicity has been identified. Barlow (1979) noted that the infrared flux varied

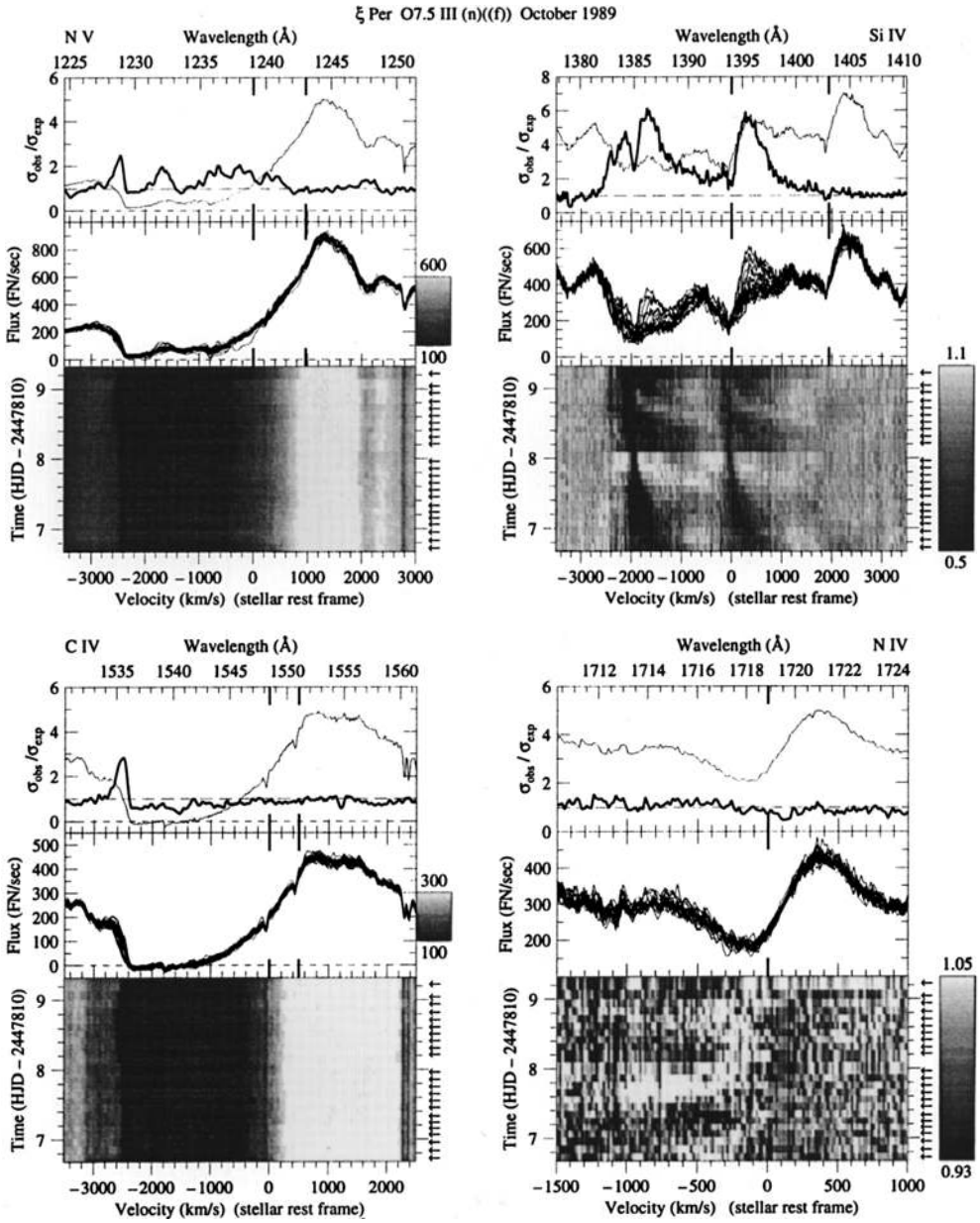

Fig. 3. As in Fig. 1: ξ Per October 1989, 23 spectra. These observations are described by Henrichs et al. (1994a). Variations occur over the full range of wind velocities (~ -100 to -2750 km s^{-1}) , from almost zero (in Si IV and N IV), to intermediate (in Si IV and N V) and the highest velocities (in N V and C IV). Note the "crossing" of DACs at about Day 8.3

substantially on at least one occasion, a circumstance that he attributed to episodic mass loss. Fullerton (1990) reported significant line-profile variability (*lpv*) in optical spectra of ξ Per, directly attributable to changes in line strength on time-scales between a few hours and a few days (similar to the UV variability, see below).

Snow (1977) reported variations in the C III lines at 1176 Å and in the Si IV resonance lines in two *Copernicus* spectra obtained four years apart. LGS detected discrete absorption components at mean velocities of -2190 and -1860 km s^{-1} in the O VI, N V, and Si IV profiles. Extensive ultraviolet observations (1978-1984) of ξ Per were carried out by Prinja et al. (1987), showing that the morphology and evolution of the variations in UV resonance lines is characterized by broad low-velocity DACs gradually evolving into narrow high-velocity DACs. The highest central velocity reached by DACs (which is a measure of v_∞) in the Si IV resonance lines was reported to be about -2250 km s^{-1}.

In Figs. 1-4 we show time series of the ultraviolet resonance lines of ξ Per observed in September 1987, October 1988, October 1989 and October 1991, respectively. The

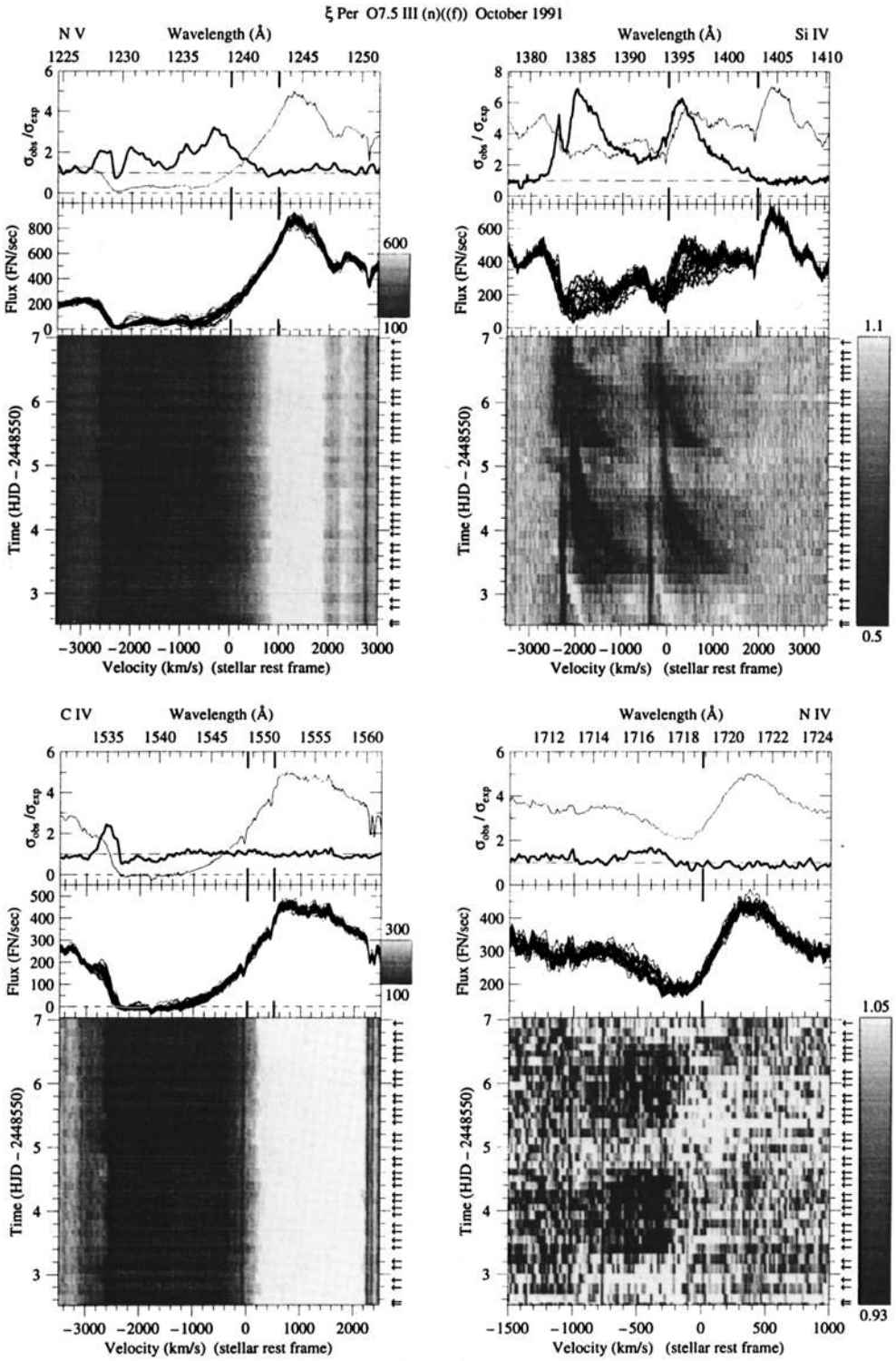

Fig. 4. As in Fig. 1: ξ Per October 1991, 36 spectra. The DAC behavior is almost identical to that observed in October 1989, except that the absorption components are now stronger than we have found previously for this star. At -2250 km s^{-1} the remainings of a DAC are visible at the start of our run and a strong DAC develops at Day 3.2 in N IV and Si IV. This DAC reaches only -1900 km s^{-1}, just like half of the components in 1988 and 1989. Indeed, the next new DAC becomes visible after about two days, followed in about half a day by a faint one, and moves up to -2150 km s^{-1}

spectra shown in the grey-scale pictures are ordered with time (increasing upwards), and the flux values are converted into levels of grey: the minimum (black) and maximum (white) cuts in flux are indicated by the side bar. For the Si IV and N IV lines the variability is better illustrated by showing quotient spectra that were obtained after division of the spectra by a reference spectrum that represents the underlying constant wind profile (cf. Paper II). The cut values were held constant for all spectral lines in a given image. The middle panels contain an overplot of the individual spectra. In the top panels the average spectrum (in case of the Si IV and N IV lines the reference spectrum) is drawn as a thin line. The σ-ratio (thick line), which is a measure of the amplitude of the variations per wavelength point, is overplotted.

The pattern of variability in ξ Per is qualitatively similar during the other campaigns. The detailed behavior of the DACs in the Si IV line differs remarkably from year to year. The amplitude of the variations (especially with respect to the N IV line) depends on the observed event. In general, a new DAC develops about every day. In the following we summarize the results in chronological order.

HKZ gave a preliminary overview of the September 1987 campaign on ξ Per and confirmed the findings of Prinja et al. (1987). The Si IV doublet exhibits the largest amplitude of variability: the absorption strength in the doublet components changes with time, due to both the evolution of DACs and variations in the steep blue edge of the P Cygni profile. In the N V profile some variations occur at low velocity, as is indicated by the σ-ratio, and are most likely related to the DACs observed in the Si IV doublet. At higher velocities the profile is saturated, prohibiting the detection of enhancements in absorption strength. The blue edges of both profiles are at about -2600 km s^{-1}. The dramatic change in the blue edge around Day 5.5 was already reported by HKZ, and is a very clear example of this kind of variability: the N V and C IV edges are at minimum velocity when a new DAC appears in the Si IV and N IV lines. The edge shifts towards higher velocity when this DAC accelerates through the Si IV profile and shifts back again to lower velocity when the DAC has reached its terminal velocity.

If the edge variability is directly related to the DAC behavior, two stages during the evolution of DACs can affect the high-velocity edge: when the DAC is accelerating towards higher velocities, the DAC can, due to its large width, "touch" the high-velocity edge before reaching the terminal velocity and subsequently "shift" the edge further to the blue. On the other hand, when a DAC feature is at its terminal velocity, it narrows in width, and diminishes the absorption at the edge velocity, so that the edge should shift back to the red. According to our interpretation of the ξ Per data, the mutual occurence of both effects might explain the edge behavior. One should keep in mind that any DAC feature detected in an unsaturated resonance line will have a much larger optical depth in a much stronger, saturated line.

The subordinate N IV line of ξ Per is varying in concert with the DACs in the Si IV resonance lines. This is most prominent in the spectra of 1989 and 1991 (Figs. 3 and 4, see also Henrichs et al. 1994a and Kaper et al. 1995a).

The results for ξ Per from the October 1989 campaign (Fig. 3) are described by Henrichs et al. (1994a). Variations occur over the full range of wind velocities, from almost zero (in the Si IV and N IV lines), to intermediate (in Si IV and N V lines) and the highest velocities (in the N V and C IV profiles) exceed the terminal velocity of the wind, measured by the asymptotic velocity reached by a DAC.

An interesting phenomenon only observed for ξ Per is the "crossing" of DACs. In the datasets obtained in October 1988, October 1989 and October 1991, a DAC in the Si IV doublet seems to settle at a velocity of -1900 km s^{-1} (e.g. Fig. 3 around Day 8.3) and is joined by a newly developed DAC. The new DAC overtakes the previous one and accelerates further to a final velocity of about -2200 km s^{-1}. The repetition of this phenomenon during other campaigns suggests that in ξ Per successive DACs can have different asymptotic velocities (-1900 and -2200 km s^{-1}). This might also have consequences for the observed edge variability: in the 1989 dataset, the N V and C IV edges are indeed at higher velocity when the DAC with a terminal velocity of -2200 km s^{-1} evolves through the Si IV profile.

The October 1991 observations (Fig. 4) show the evolution of DACs in the Si IV doublet (accompanied by additional absorption in the N IV line) in great detail. The 36 spectra include the strongest absorption components we have encountered for this star; the absorption enhancements in the N IV line are very pronounced and last about one day. Clearly, the relatively long time coverage during this campaign provides better insight into the evolution of DACs. The shortward doublet component of the N V profile shows some signs of the development of the first DAC at intermediate velocities (~ -1000 km s^{-1}). The steep blue edges of the C IV and N V profiles change in concert, but a connection with the variations in the other lines (i.e. the DAC behavior) at lower velocities is not straightforward. From our 1989 observations we would predict that the edge in N V and C IV is at higher velocity around Day 6, when a "-2200" DAC evolves through the Si IV profile. The 1991 dataset does not disprove this prediction, but a firm conclusion is hard to draw. The great strength of the absorption components (and correspondingly their long lifetime) results in the simultaneous presence of both "old" and "new" DACs. This shows that objects like ξ Per with a rapid variability pattern are in fact not good candidates to reveal a clear relation between DAC behavior and absorption edge variability.

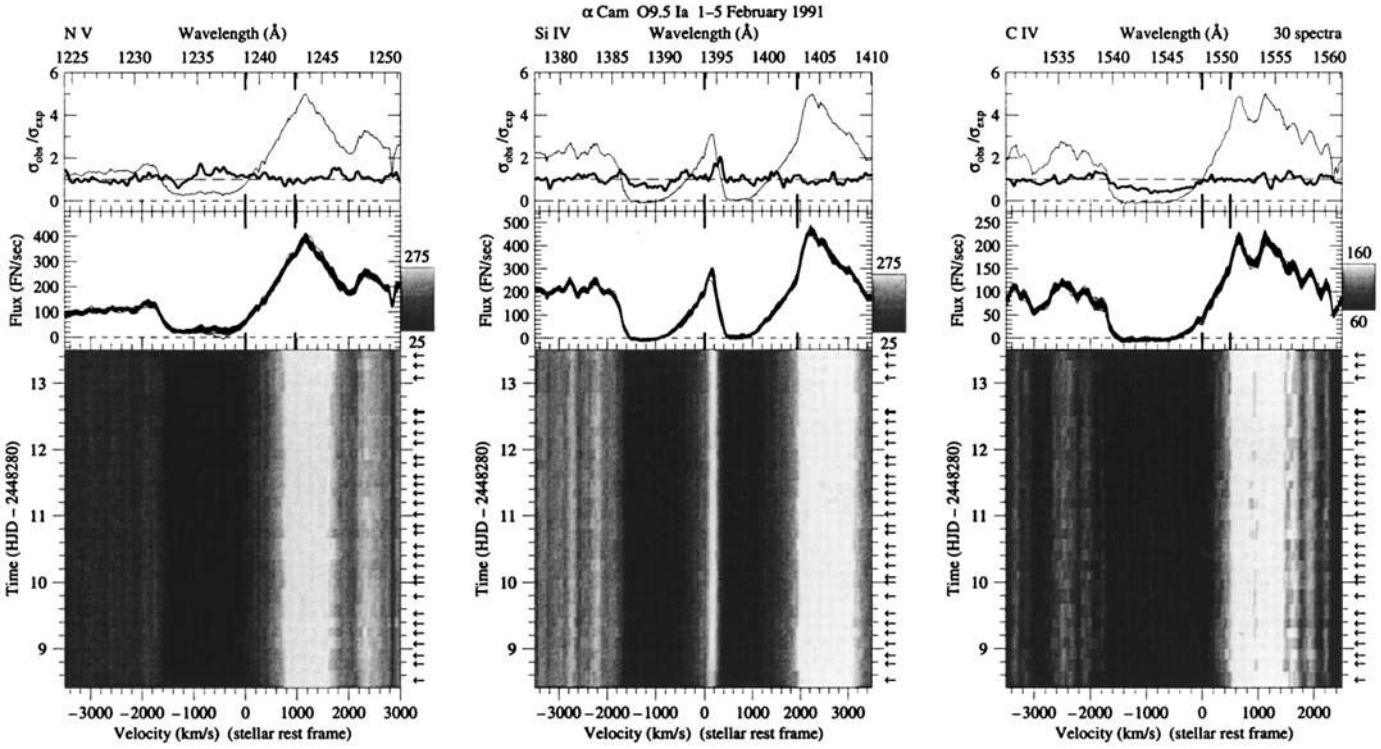

Fig. 5. As in Fig. 1: α Cam O9.5 Ia in February 1991. The resonance lines of α Cam are heavily saturated and do not vary significantly. This supergiant is the only O star in our sample that does not show variability in its ultraviolet spectrum

4.2. *HD 30614 (α Cam) O9.5 Ia*

The supergiant α Cam is a runaway star (cf. Gies 1987; Blaauw 1992) with presumed parent the young open cluster NGC 1502 at a distance of about 1 kpc. The high relative speed of α Cam in the cluster (about 48 km s^{-1}) causes a bow-shock effect in the interstellar medium (De Vries 1985). This bright star has been monitored extensively for variability in the optical wavelength domain. Ebbets (1980, 1982) found dramatic night-to-night changes in the shape of the low-velocity part of the broad emission feature at Hα, as well as subtle *lpv* in He I 6678 Å. Fullerton (1990) reported significant variability in all lines he studied in the optical spectrum of α Cam, where the strong He I line at 5876 Å exhibits the largest amplitude. Hayes (1984) and Lupie & Nordsieck (1987) detected systematic, but aperiodic, variations in optical continuum polarimetry of α Cam; they attributed these fluctuations to "puffs" of matter in the stellar wind.

Gathier et al. (1981) reported narrow absorption components in Copernicus data of the Si III, Si IV, N V, and O VI lines, but gave all their measurements low weight. Lamers et al. (1988) presented observational evidence for variations in high-resolution IUE spectra of α Cam obtained in September 1978. Changes were reported in the strong and saturated resonance lines, both in emission and in absorption at three velocity regions near −1800, −700, and +700 km s^{-1}. The authors interpreted the variations as a result of the clumpiness of the stellar wind. However, PH could not confirm the presence of these features at the velocities reported in the same dataset.

We observed α Cam during five days in February 1991. The resonance lines of this supergiant are strongly saturated and the P Cygni emission has a triangle-shaped peak (Fig. 5). Except for small variations at the blue edge of these profiles (see the σ-ratio in the top panels of Fig. 5) we could not detect significant variability. The position of the blue edge for the three resonance lines is the same, namely −1700 km s^{-1} (measured at half intensity of the estimated continuum level). The ultraviolet observations were covered by high-resolution optical spectroscopy of the Hα line (Kaper et al. 1992) of α Cam; like Ebbets, we found large changes in the line profile from night to night, and also within a night. But, as shown in this paper, these variations in the base of the wind are not reflected in the UV resonance lines.

4.3. *HD 34656 O7 II(f)*

HD 34656 is the faintest star in our sample, and was included because Fullerton et al. (1991a) tentatively identified the *lpv* observed in optical spectra of this star with a pulsation in the radial fundamental mode, which is exceptional for such a star. He compares the pulsational

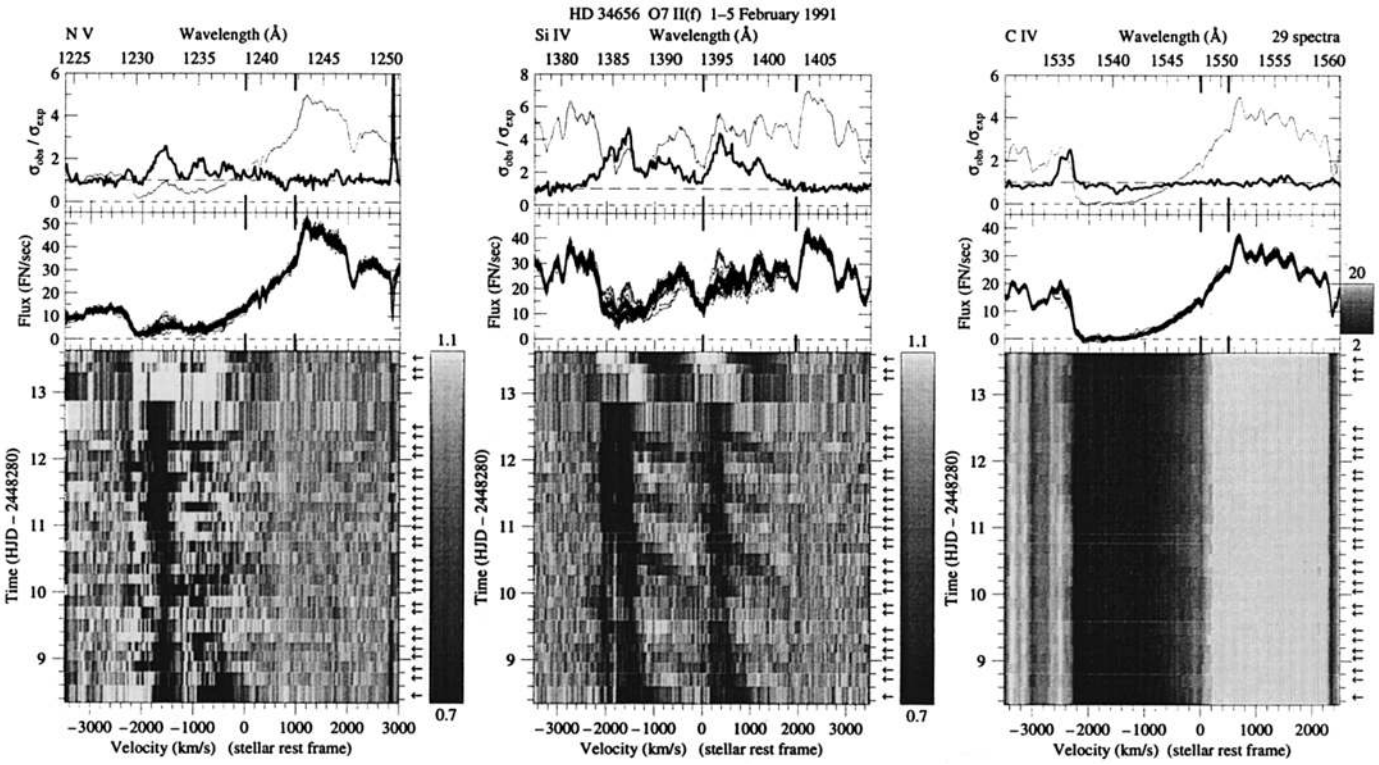

Fig. 6. As in Fig. 1: HD 34656 O7 II(f) in February 1991. Quotient spectra are used for the grey-scale panels of the N v and Si iv profiles. The Si iv line exhibits the migration of several DACs on a timescale of about 1 day. Apart from that, a gradually varying strong absorption component is present at higher velocities. This component is also found in the N v line. The detailed variability pattern is very complicated. Although the maximum velocity reached by these DACs is about -1900 km s^{-1}, wind variability extends from almost zero to -2600 km s^{-1}. The C iv edge slightly varies around -2400 km s^{-1} as reflected by the σ-ratio

behavior of HD 34656 with that of a β Cephei star, although the found period of 8.21 hours seems to be quite long. Conti (1974) noted the presence of a peculiar broad emission reversal in the center of the Hα line. HP mention the presence of a narrow DAC in an archival IUE spectrum of HD 34656.

We observed the star during the February 1991 campaign (Fig. 6). The Si iv line clearly shows the migration of several DACs on quite a short timescale (about 1 day). The maximum velocity reached by these DACs is about -1900 km s^{-1}. The morphology of the variations is, however, very complicated. On top of the "rapid" DAC pattern additional absorption seems to be superposed. Wind variability extends from almost zero velocity to -2600 km s^{-1}, i.e. the full range of velocities in the stellar wind. The N v doublet is close to saturation, but shows clearly the gradually varying additional absorption component also seen in Si iv. This absorption around ~ -1700 km s^{-1} is strongest between Day 11 and 13 in both the Si iv and the N v line. The C iv edge shows slight variations around -2400 km s^{-1}, which do not seem to be present in the blue edge of N v.

4.4. *HD 36861 (λ Ori A) O8 III((f))*

This star is member of a visual binary (separation about 5 arcsec). Star A (our target) is considered spectroscopically single (Garmany et al. 1980). Although star B would fall within the IUE large aperture, its contribution is negligible. The optical spectra indicate the presence of line-variability (Jarad et al. 1989; Fullerton 1990). Snow (1977) detected a strong narrow component in the N v (and less clear in the Si iv) lines at -2000 km s^{-1} in *Copernicus* spectra. LGS found a similar component in the O vi resonance doublet. PH reported variable DACs in the ultraviolet N v and C iv profiles of λ Ori around -2000 km s^{-1}. They found strong evidence that the strengths of the DACs in these two ions are correlated.

Also in our dataset of λ Ori obtained in November 1992 (Fig. 7), a strong displaced absorption component (see middle panels) is present at -2000 km s^{-1} in both N v and Si iv (although in the latter less pronounced). This component remains unchanged during the full observing period of five days. The absorption in the C iv line also seems to be enhanced around this velocity. The *persistent* absorption component could be a DAC at its final velocity. The σ-ratio indicates some variability at the

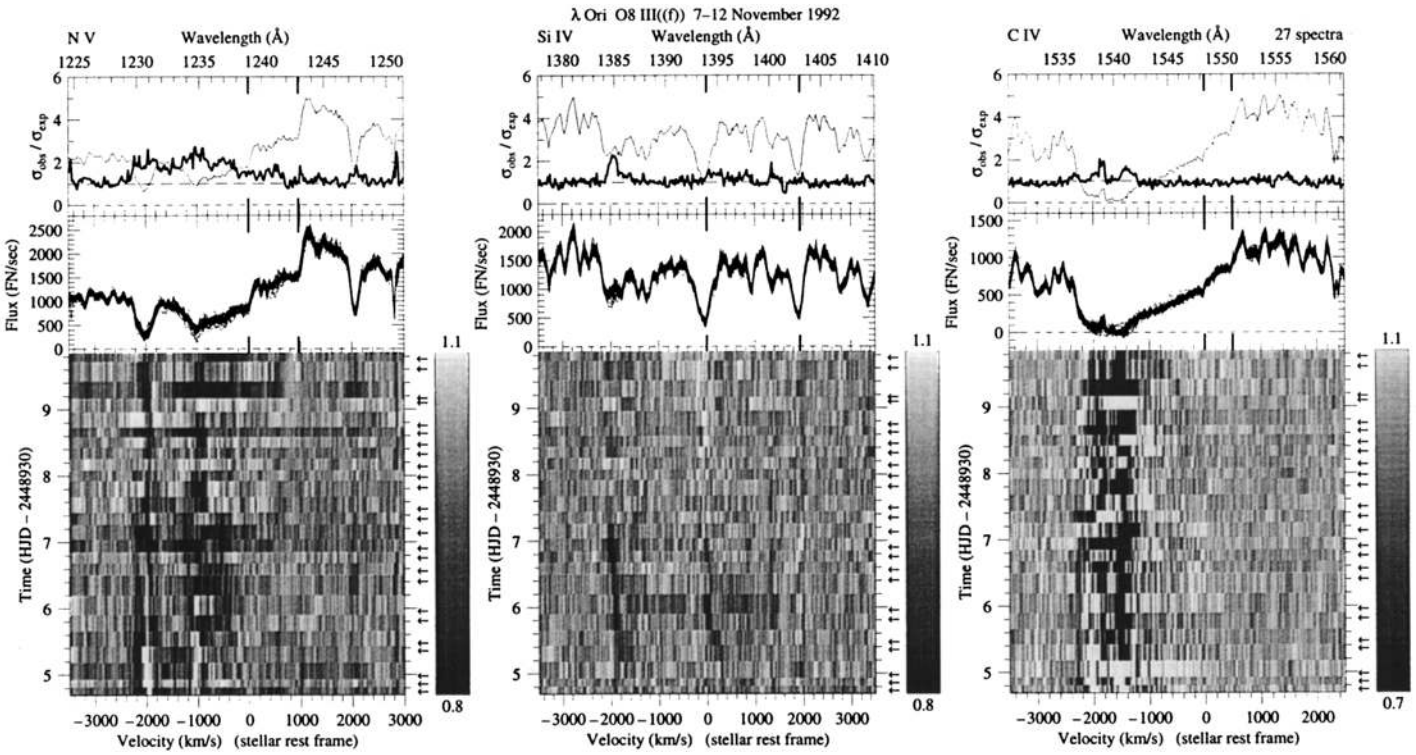

Fig. 7. As in Fig. 1: λ Ori O8 III((f)) in November 1992. The grey-scale panels show quotient spectra that better illustrate the variability. A *persistent* absorption component is present at −2000 km s^{-1} in the N V and Si IV profiles (see middle panels). The appearance of these spectra is very similar to that of 15 Mon (cf. Fig. 9). A weak absorption component appears in the Si IV doublet, accelerating from about 1700 to 2000 km s^{-1}, i.e. towards the persistent component

position of the absorption components. The grey-scale panels display quotient spectra to better illustrate this variability. In the Si IV doublet a weak migrating absorption component is present, accelerating from about −1700 to −2000 km s^{-1}, i.e. towards the persistent absorption component. A pattern of variability could not be discovered in the N V and C IV lines. The recurrence timescale of DACs is most likely longer than five days for this star. The spectrum is very similar to that observed for 15 Mon (see below).

4.5. *HD 37742 (ζ Ori A) O9.7 Ib*

ζ Ori, the most eastern star in Orion's belt, is also a member of a wide visual binary system (separation about 2 arcsec), and spectroscopically single according to Garmany et al. (1980). It has been subject to extensive monitoring for variability. Ebbets (1982) detected large changes in the shape of the low-velocity part of the broad emission feature at Hα. These changes were accompanied by significant changes in line strength. Fullerton (1990) found some evidence for *lpv* in optical spectra of ζ Ori.

In *Copernicus* spectra of this star Snow (1977) observed variable emission in the C III and N V profiles. He detected a narrow absorption feature at a displacement of −1630 km s^{-1} in N V, which was also present in O VI, Si III, and Si IV, according to LGS. PH identified DACs in the N V resonance lines, while both Si IV and C IV were saturated at velocities corresponding to the expected positions of the DACs.

In late September 1992 (i.e. two months before our observations) a rise in X-ray flux from ζ Ori by about 30% over a period of 48 hours was observed by the ROSAT satellite (Berghöfer & Schmitt 1994). Although hot stars are known soft X-ray sources, this kind of X-ray variability is not commonly observed. Since the X-rays are most likely produced in the stellar wind, this suggests that the observed X-ray flare is related to a particular event in the wind.

The time series of the wind lines of ζ Ori resulting from our November 1992 campaign are shown in Fig. 8. The grey-scale panels of both the N V and the Si IV line contain quotient spectra. The N V line shows the development of a DAC in the N V profile at Day 7.5, starting at a velocity of about −800 km s^{-1}. This component accelerates during the last two days of our observations towards the velocity of the steady absorption component at −1700 km s^{-1}. The DAC does also show up in the Si IV doublet, but here, and in the C IV profile, the edge variability is more pronounced. The strange features in

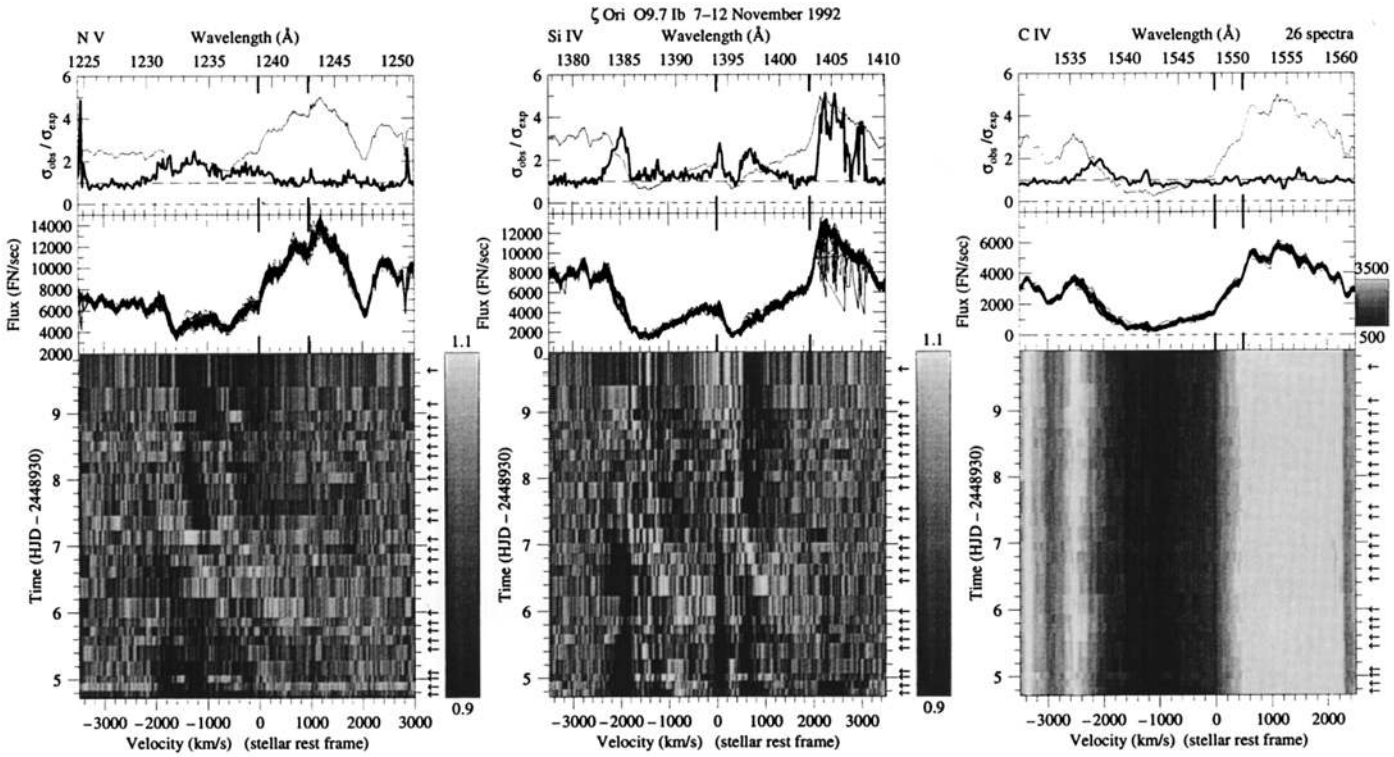

Fig. 8. As in Fig. 1: ζ Ori O9.7 Ib in November 1992. The grey-scale panels of both the N v and the Si iv line contain quotient spectra. At Day 7.5 a DAC appears in the N v doublet and slowly accelerates through the profile. A similar feature can be found in the Si iv doublet. In the Si iv and C iv P Cygni lines the edge variability (around -2000 km s^{-1}) is more pronounced

the emission peak of some Si iv spectra are artifacts of unknown origin, perhaps caused by saturation of the camera in this part of the spectrum (ζ Ori is a first magnitude star!). Close inspection shows that at the beginning of our campaign, at Day 4.5, additional absorption is present around -1400 km s^{-1} in the N v line. This means that we can estimate a lower limit for the recurrence timescale of DACs for this star, which is about three days.

Changes in the "steep" edge occur in all three profiles. These changes take place during the first half of our observations, when additional absorption is present at lower velocities. From this single event it is impossible to discover any relation between edge variability and DAC behavior in this star, which does, however, not exclude that these two manifestations of variability are physically related.

4.6. *HD 47839 (15 Mon) O7 V((f))*

This O main sequence star (also known as S Mon) has been subject to extensive observational studies. In our study, we have considered 15 Mon to be a single star. Recently, however, Gies et al. (1993) discovered a speckle binary companion to 15 Mon. Optical and ultraviolet spectroscopy suggests that the star is also a spectroscopic binary with a period of 25 years and a large eccentricity. Gies et al. derive masses of 34 and 19 $M_\odot$ for the primary and secondary (probably an O9.5 Vn star), respectively. Fullerton (1990) considers the optical line profiles to be constant in shape, but the spectrum of 15 Mon may vary on a timescale longer than covered by his observations. This star emits X-rays and the X-ray flux is found to change significantly over intervals as short as 5 days (Snow et al. 1981).

The N v and O vi resonance lines in *Copernicus* spectra of 15 Mon contain strong narrow absorption components, shortwardly displaced by about 2000 km s^{-1} (Snow 1977, LGS). Grady et al. (1984) accounted for variations in $v_{\rm edge}$ in modeling the ultraviolet P Cygni profiles, but PH did not include this and still obtained good fits. The changes near the blue edge of the profiles are considered by them to be due to changes in width and central velocity of DACs at lower negative velocities.

The UV spectrum of 15 Mon is similar to that of λ Ori, described above. Also in this star a strong persistent absorption component (see middle panels) is present in the N v and C iv doublets at -2000 km s^{-1}. The Si iv line is probably too weak to show wind absorption and we see only the photospheric components. The variability as reflected by the σ-ratio also looks similar to that observed for λ Ori but the amplitudes of variability are even smaller. Although the small variations in the N v line could be due to bad flux calibration in this part

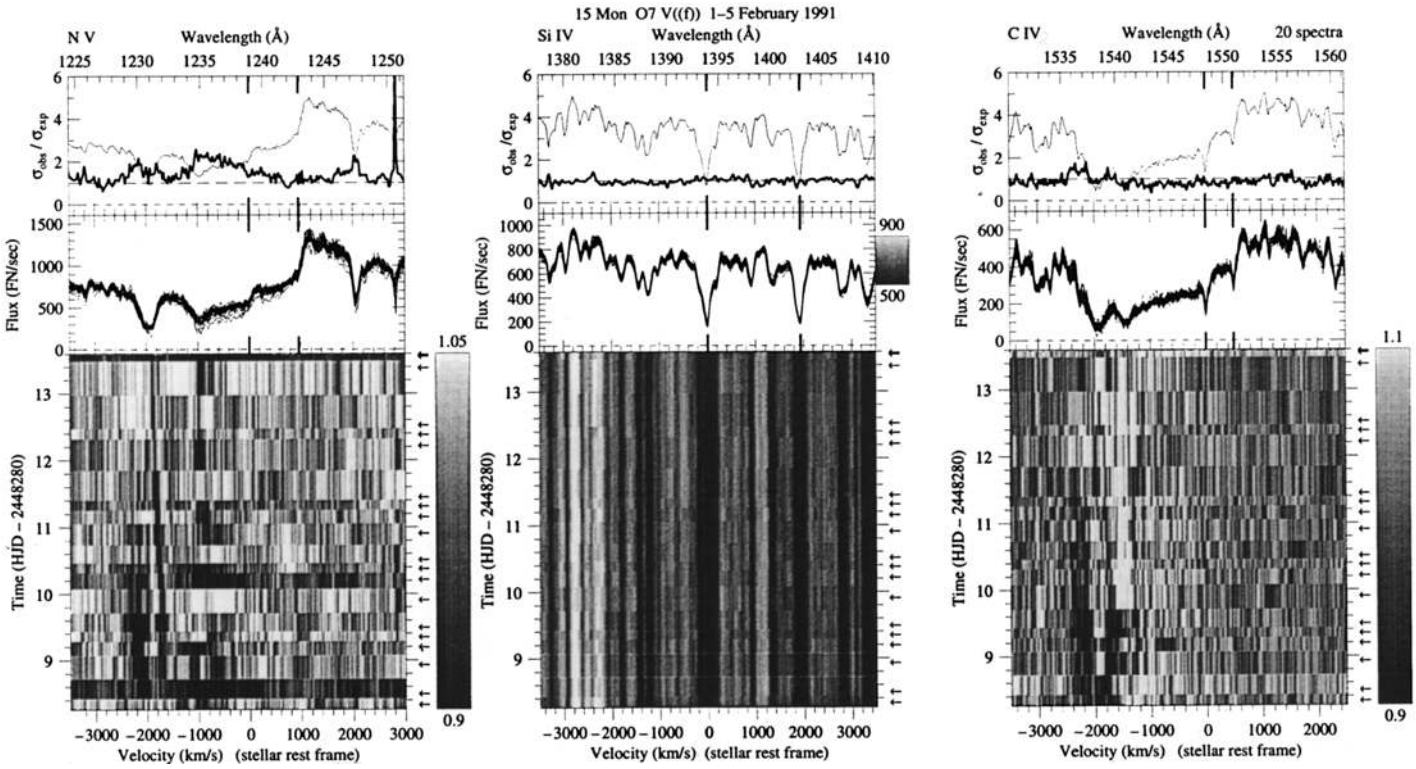

Fig. 9. As in Fig. 1: 15 Mon O7 V((f)) in February 1991. The N v and C iv panels display quotient spectra. At -2000 km s^{-1} a persistent absorption component is present in the N v and C iv lines (see middle panels). A very narrow absorption feature travels through the N v, and less clear, through the C iv lines, in the direction of the persistent component. The UV resonance lines are very similar to those in the spectrum of λ Ori (Fig. 7), which also includes a persistent component at -2000 km s^{-1} in the N v and C iv lines

of the spectrum, some enhancements in the blue-shifted absorption seem to occur in the profile occasionally. A very narrow absorption feature travels through the N v, and less clear, through the C iv lines, in the direction of the persistent component, as revealed by the quotient spectra contained in the grey-scale panels.

4.7. *HD 203064 (68 Cyg) O7.5 III:n((f))*

The runaway star 68 Cyg is associated with a ring nebula (Alduseva et al. 1982) and is member of the Cyg OB7 association (Humphreys 1978). The measured $v \sin i$ of 274 km s^{-1} indicates that this giant star is rotating rapidly. The broad photospheric lines do show statistically significant and qualitatively similar line profile variations (Fullerton 1990). The strongest variations in the form of transient absorption enhancements occur in the stronger optical lines, like the He i triplet at 5876 Å, He ii 4686 Å, and Hα.

The regular variability of the UV resonance lines of 68 Cyg in the August 1986 dataset (see below) has been independently analyzed by Prinja & Howarth (1988). They conclude that the DACs in the wind of 68 Cyg are not due to "shells" or "puffs" of matter, but instead arise from material passing through perturbations in the flow, which can be illustrated in terms of spirally wound-up streams. Kaper et al. (1990) reported the remarkable constancy of the DAC pattern over many years. The first results from the September 1987 campaign of simultaneous optical and UV observations of 68 Cyg were presented by Fullerton et al. (1991b). There was only one indication that photospheric and wind variability in this star might be related, namely a simultaneous decrease in $v_{\rm edge}$ of the ultraviolet C iv wind line and the equivalent width of the He ii line at 4686 Å. This helium line is partly formed at the base of the wind.

In Fig. 10 we present the timeseries of ultraviolet spectra obtained in August 1986. The variations in the Si iv doublet (shown by quotient spectra) are described by Prinja & Howarth (1988). The time resolution is insufficient to resolve rapidly evolving DACs in the early part of the timeseries; in the later part three events can be recognized. The first two are separated by half a day, followed by a third after another day. The asymptotic velocity of the DACs is about -2350 km s^{-1}. The characteristic pattern formed by these three events also appears in the October 1988 observations (see Fig. 12).

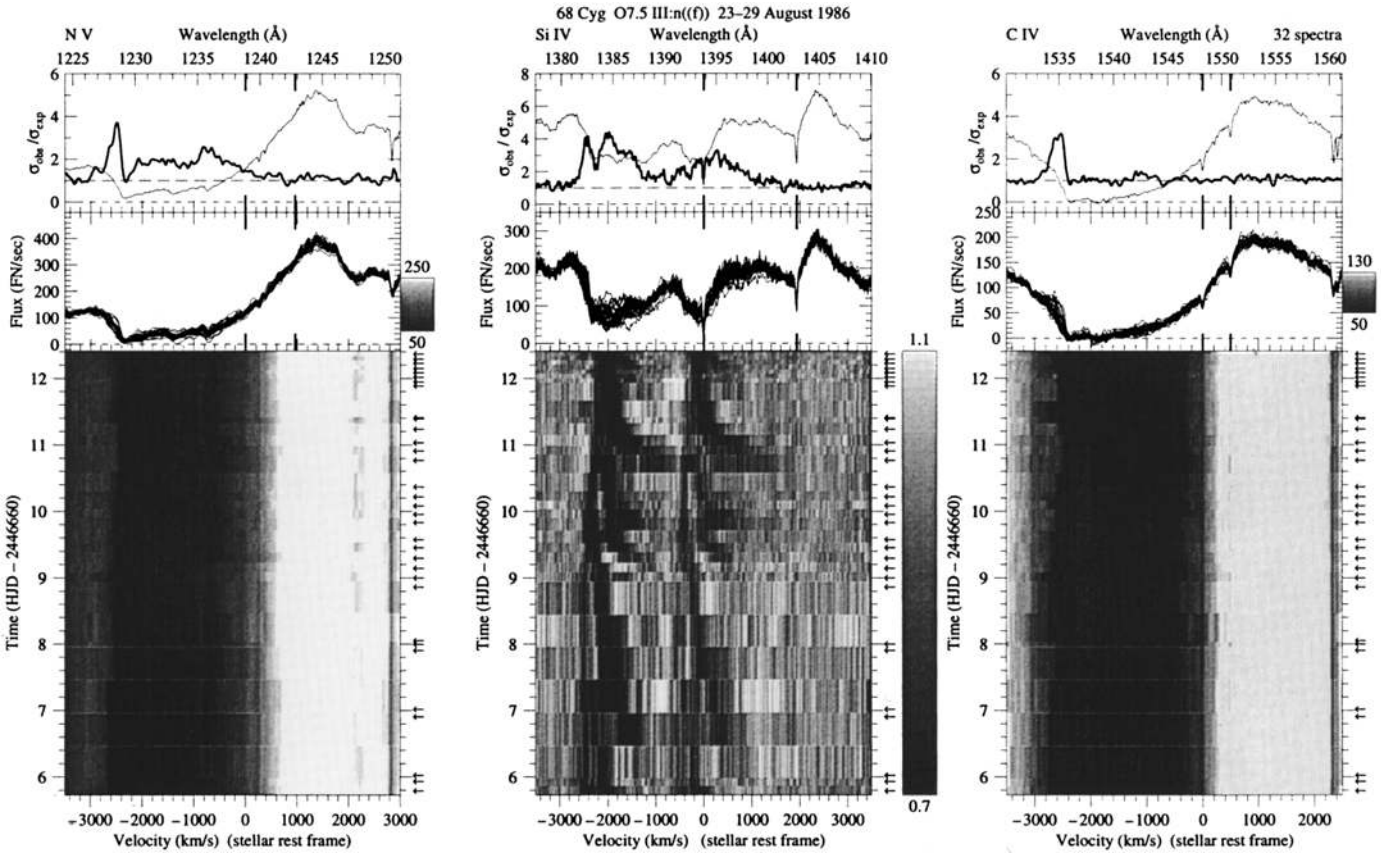

Fig. 10. As in Fig. 1: 68 Cyg O7.5 III:n((f)) in August 1986. The evolution of DACs in the Si IV doublet (note the quotient spectra) is described by Prinja & Howarth (1988). In the upper part of the time series three events are found: the first two are separated by half a day, followed by a third one a day later. The DAC's asymptotic velocity is about -2350 km s^{-1}. The formed pattern can be recognized in the October 1988 dataset. The extent of variability in the Si IV doublet, as indicated by the σ-ratio, ranges from about -800 to -2600 km s^{-1}. The N V doublet is variable over the same range of wind velocities, but here the edge variability is most pronounced, which is even more evident in the C IV P Cygni profile

The extent of variability in the Si IV doublet, as indicated by the σ-ratio, ranges from about -800 to -2600 km s^{-1} (cf. Table 4). The N V doublet is variable over the same range of wind velocities (-800 to -2700 km s^{-1}), but here the edge variability is most pronounced, with maximum amplitude at -2500 km s^{-1}. The edge variability in the C IV P Cygni profile (-2400 to -2800 km s^{-1}) is even more evident. Howarth & Smith (1995) find significant variability in a range from -800 to -2730 km s^{-1} for Si IV, -1800 to -2930 km s^{-1} for C IV, and ≥ -1300 to -2755 (-800 to -2600) for N V, considering the yearly datasets. Combining all the available spectra they find low-velocity limits of -750, -1270, and 0 km s^{-1} for Si IV, N V, and C IV, respectively. This shows that their results are consistent with ours, except for the low-velocity limit of the C IV variability. This might be due to the fact that our method to detect variability overestimates the noise at low flux levels, caused by the scarcity of calibration points in this flux range (cf. Henrichs et al. 1994a).

The N V and C IV edges are at minimum displacement during the second half of the observations; a similar behavior is observed for the Si IV edge. At that epoch a Si IV DAC at its terminal velocity (from about Day 9 on) starts fading in strength.

In September 1987 the migration of DACs in the Si IV profile is quite regular; from Fig. 11 it is obvious that all DACs reach the same asymptotic velocity (approximately -2350 km s^{-1}), and provide strong support for the idea that this velocity corresponds to the terminal wind velocity (HKZ, Prinja et al. 1990). The velocity corresponding to the blue edge in the saturated C IV and N V lines is about 350 km s^{-1} larger. A new DAC appears about every 1.3 days, but between the DAC events at Days 5.4 and 6.8, a DAC develops half a day before the appearance of the latter DAC.

The DAC recurrence timescale is defined as the distance in time between two successive DACs. In this case it is not possible to determine the recurrence timescale unambiguously. The characteristic timescale of the

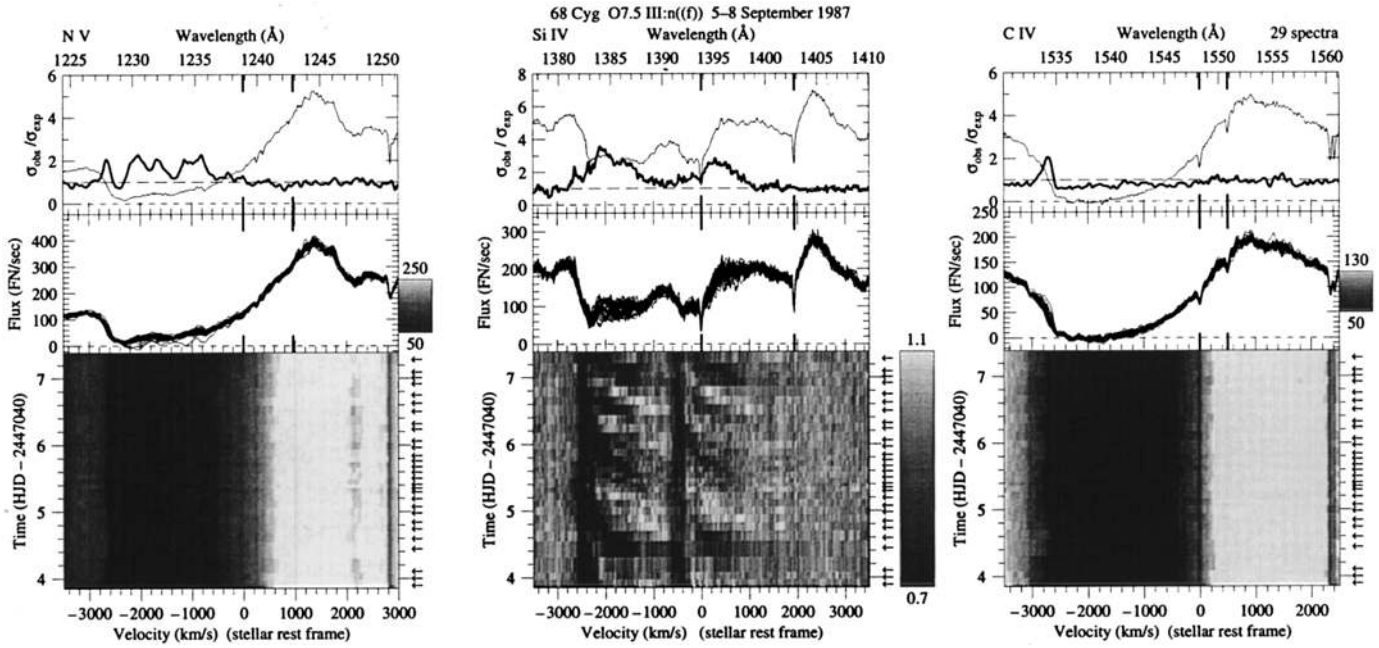

Fig. 11. As in Fig. 1: 68 Cyg O7.5 III:n((f)) in September 1987. The migration of DACs in the Si IV profile is very regular. Each DAC reaches the asymptotic velocity of about -2350 km s^{-1}. The velocity corresponding to the blue edge in the saturated C IV and N V lines is some 350 km s^{-1} higher. The recurrence timescale of DACs is about 1.3 days, but in between the DAC events at Days 5.5 and 6.8, a DAC develops half a day before the appearance of the latter DAC

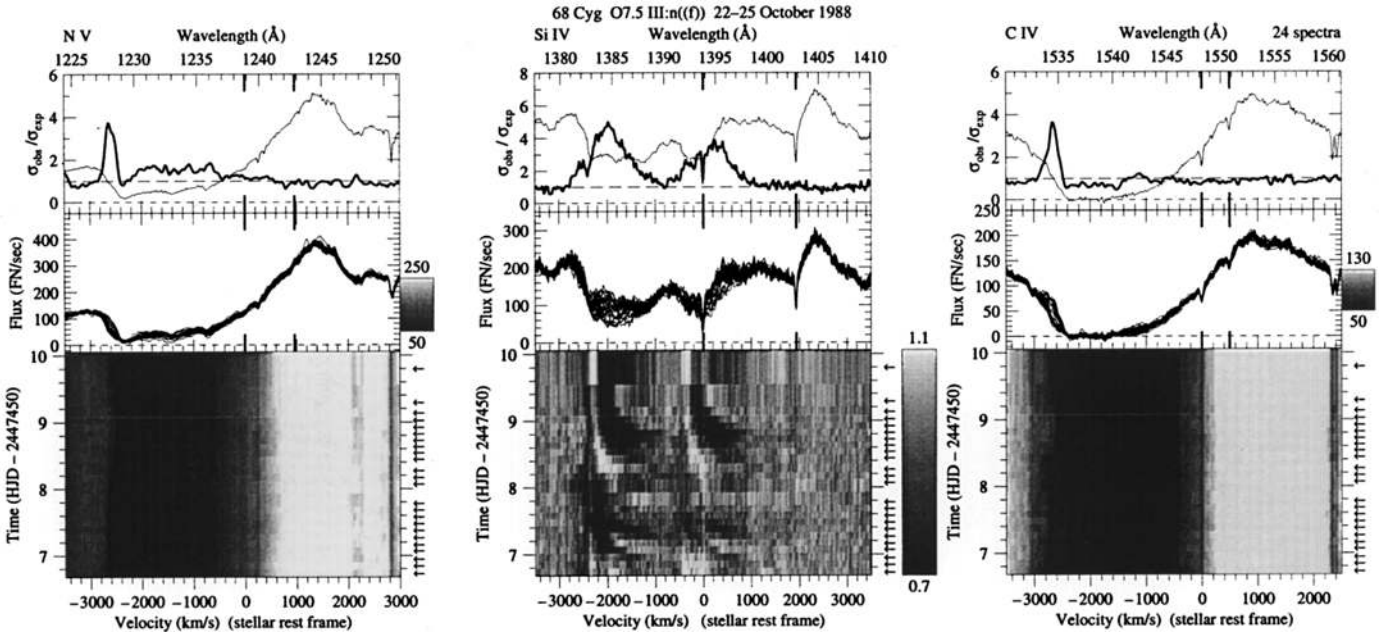

Fig. 12. As in Fig. 1: 68 Cyg O7.5 III:n((f)) in October 1988. A similar characteristic pattern (see Fig. 10) of DAC variability in the Si IV doublet of 68 Cyg is clearly recognized. The amplitude of variability given by the σ-ratio is at its maximum, both in the Si IV line because of migrating DACs and in the saturated C IV line due to the varying steep edge. The edge of C IV is at minimum displacement (Day 9) when a narrow component at its terminal velocity is about to disappear

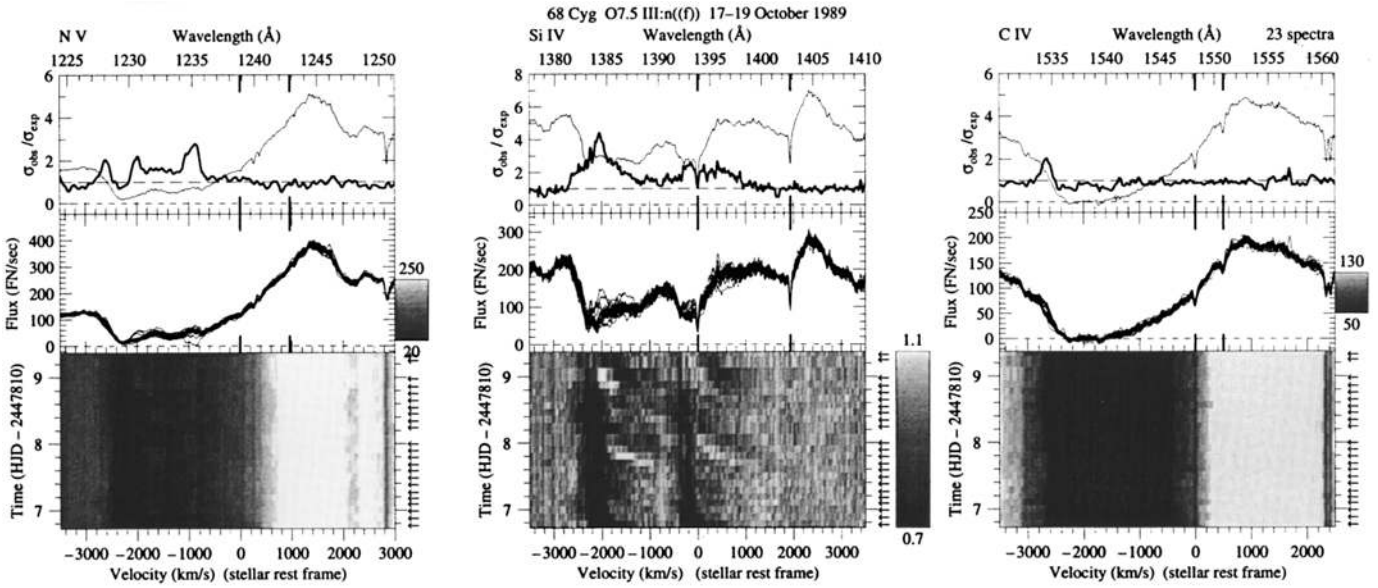

Fig. 13. As in Fig. 1: 68 Cyg O7.5 III:n((f)) in October 1989. In this relatively short time series the global pattern of variability has not changed, but the amplitude of the variations is smaller than in the previous years

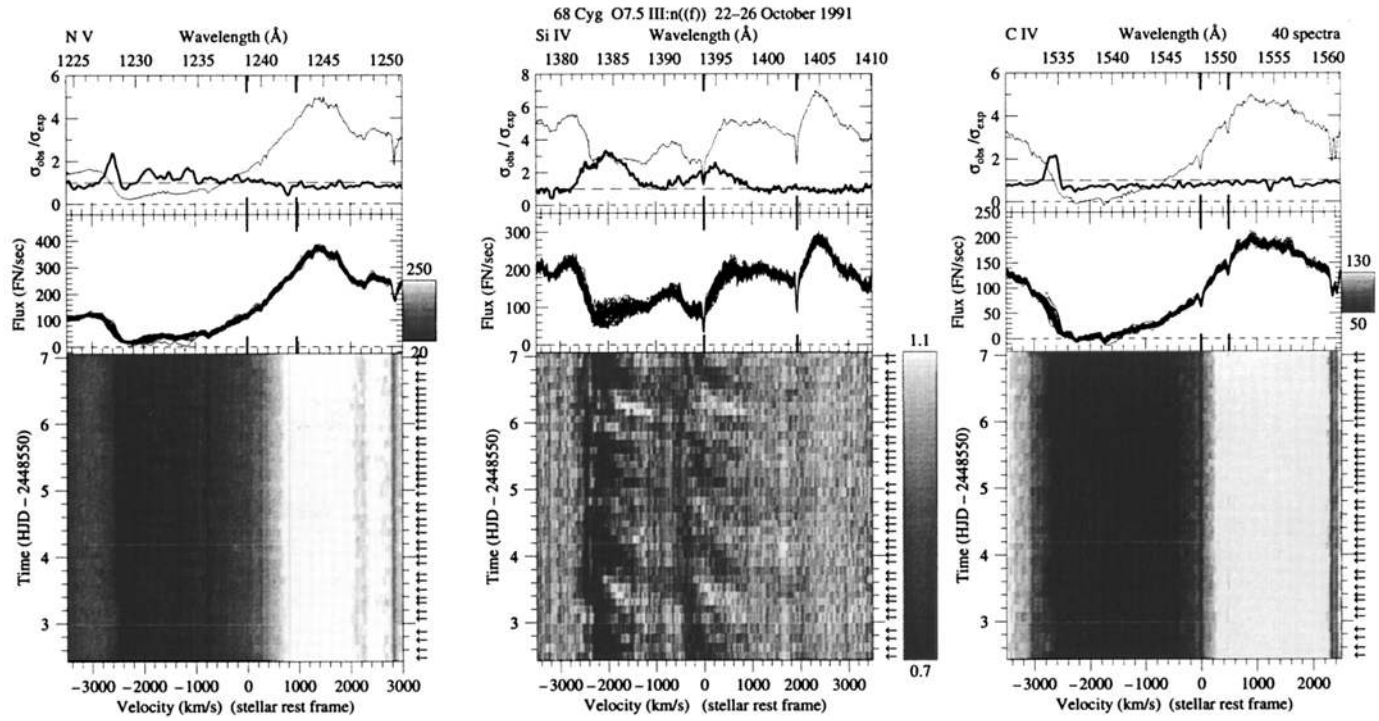

Fig. 14. As in Fig. 1: 68 Cyg O7.5 III:n((f)) in October 1991. This year the variations have the lowest amplitude, but DACs appear very regularly, the stronger ones about every 1.3 day. The steep edges of the N v and C iv profiles vary in concert; similar variations observed in the edge of the Si iv profile seem to be related to the DAC behavior

variability might be better defined here by the time elapsed between two successive *strong* DACs, which is about 1.3 days. Taking into account the other datasets, one has to conclude that sometimes a weaker absorption component appears within half this time interval. A similar conclusion can be drawn from the UV observations of ξ Per and 19 Cep (below). Thus, in these cases it is not the recurrence timescale of individual DACs that best describes the regularity of the phenomenon, but rather the repetition timescale of a certain DAC "pattern". In Paper II we show that a Fourier analysis applied to the present dataset gives maximum power at a period of 1.33 days, which gives support to our alternative definition for the characteristic timescale of wind variability. In paragraph 5.3 we return to this point.

Although the variations take place within the same range as in August 1986 (and later years, see below), the *amplitude* of variability clearly changes over the years. Again the edge of the N V and the C IV profile gradually changes its position, corresponding to the absorption changes at high-velocity in Si IV.

The characteristic pattern of DAC variability in the Si IV doublet of 68 Cyg is clearly recognized in the observations of October 1988 (Fig. 12). In this year the amplitude of variability is at its maximum, both in the Si IV line in the form of migrating DACs and in the saturated C IV line due to the varying steep edge. The edge of C IV is at minimum displacement when a narrow component at its terminal velocity is getting weaker. The 1986 dataset provides a similar trend. The time sequence of October 1989 is rather short (2.5 days) and allows the detection of four DAC events, which means that about every 0.6 day a new DAC develops. The edge of C IV and N V is changing with time; the P Cygni emission is constant, which is the case for all other timeseries included in this study as well.

Our most recent campaign on this star in October 1991 (Fig. 14) resulted in a very homogeneous series of spectra. From this series we can confirm that the strong DACs appear every 1.3 day, with sometimes the occurrence of a weak component in between. The steep edges of the N V and C IV profiles vary in concert; similar variations observed in the edge of the Si IV profile seem to be related to the DAC behavior.

4.8. *HD 209975 (19 Cep) O9.5 Ib*

This supergiant is a member of the Cep OB2 association. Very little is known about its variability; Ebbets (1982) found changes in the absorption strength of Hα, which were confirmed by recent Hα monitoring of this star by Kaper et al. (1995a). Fullerton (1990) detected significant variability in the He I 5876 Å line. The projected rotational velocity $v \sin i$ of 19 Cep is 75 km s^{-1}, which results in a rotation period of about 12 days (if the rotation axis is inclined by 90 degrees with respect to the line of sight, see Sect. 5).

HKZ and Prinja (1988) presented the relatively slow migration of a DAC in the Si IV resonance doublet, obtained during the August 1986 campaign. Here we further show the timeseries of the N V and C IV P Cygni lines. From Fig. 15 we conclude that both the Si IV and the N V P Cygni line (shown are quotient spectra) exhibit significant changes in the blue-shifted absorption part from about -500 up to -2300 km s^{-1}, with maximum amplitude around -1500 km s^{-1}. A strong and broad DAC (with initial width more than 500 km s^{-1}, cf. Paper II) migrates through the almost saturated Si IV and N V lines and accelerates slowly towards its asymptotic velocity (-1750 km s^{-1}) during the following 5 days. This is the velocity reached by the narrow DAC present since the start of the observations. The blue edge of the three shown profiles is varying, being at minimum displacement at Day 10 when the narrow DAC at the terminal velocity disappears. The timescale of variability for 19 Cep is much longer than for ξ Per or 68 Cyg. The slower acceleration of DACs seems to be accompanied by a longer time interval before recurrence. For the latter we can in this case only provide a lower limit of about 5 days.

Because of the long timescale of variability in August 1986, we could expect beforehand that the timeseries obtained in September 1987 (Fig. 16) and October 1988 (Fig. 17) are too short to witness a complete evolution cycle of a DAC. Although some DACs seem to be present at (or close to) their terminal velocity in the Si IV and N V doublets, only in 1988 the development of a new DAC (but by no means as strong as the DAC in 1986) is detected. No variations are found in the blue edge of the saturated C IV profile in 1987, but in 1988 we note significant changes: again the edge is at minimum displacement when a high-velocity component is getting weaker. The saturation of the N V and Si IV doublets in August 1986 results from the presence of a strong DAC, assuming that in 1987 and 1988 these profiles are not saturated.

The October 1991 observations were covered by simultaneous optical observations (cf. Kaper et al. 1995a). In the center of the Hα absorption line a strong and variable emission component is found, just before the appearance of a moderately strong DAC in the Si IV line at Day 4 (Fig. 18). Close to the end of the campaign we note an enhancement in absorption at intermediate velocities, possibly the appearance of a new DAC around Day 6.5. From these observations we would then conclude that the recurrence timescale of DACs is 2.5 days, i.e. half of the 5-day period we find in November 1992 (see below and Fig. 19). In the case of ξ Per and 68 Cyg we sometimes encountered weak DACs occuring in between two successive strong absorption components. In October 1991 we might have observed a similar behavior for 19 Cep.

Our last campaign on 19 Cep was organized in November 1992. In Fig. 19 the development of a DAC at Day 5 is observed, which is similar to the DAC in 1986 but not

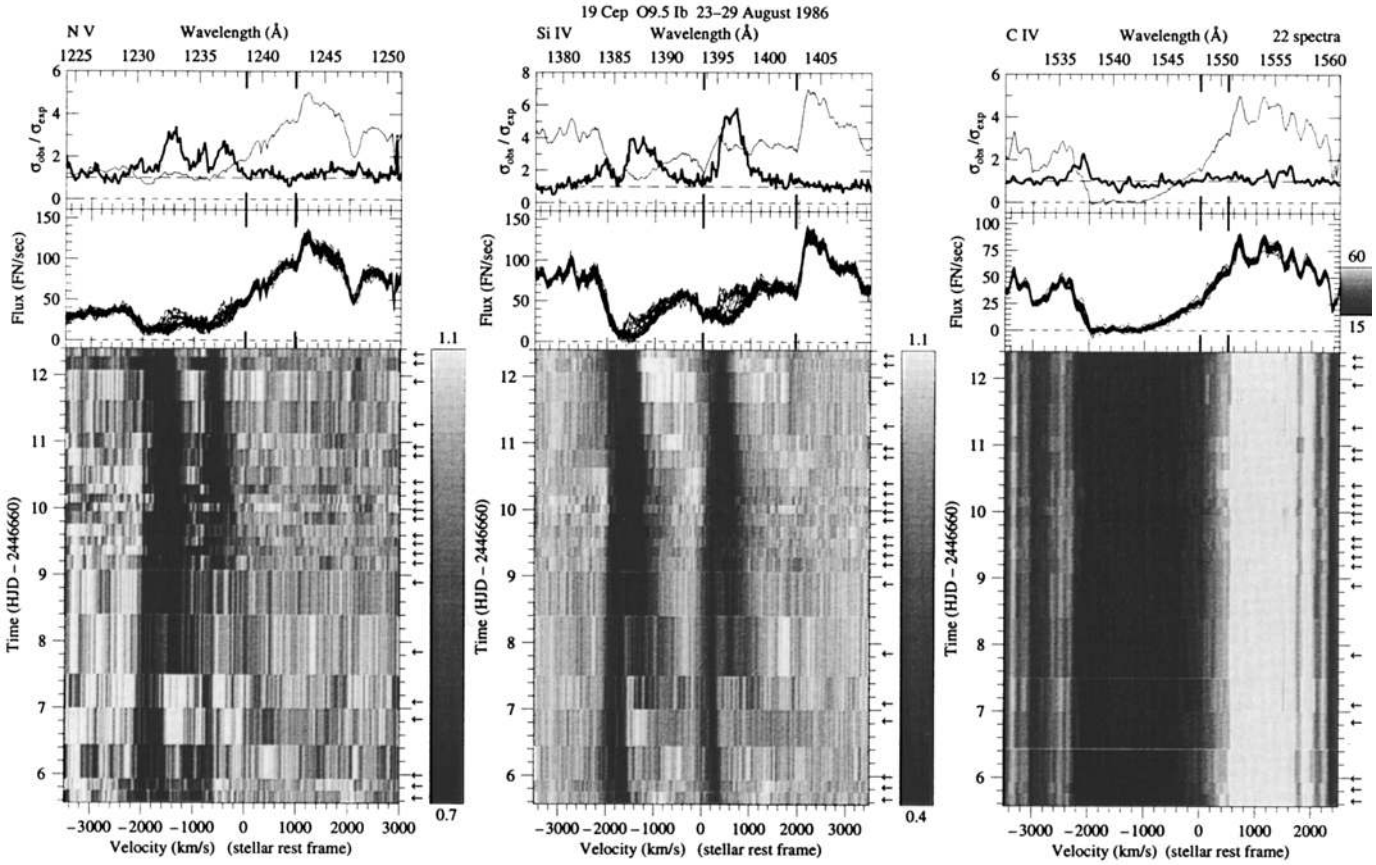

Fig. 15. As in Fig. 1: 19 Cep O9.5 Ib in August 1986. The slow rotator 19 Cep exhibits a slowly migrating and very strong DAC in both the N v and the Si iv UV resonance lines (shown are quotient spectra). The DAC present since the start of the observing campaign has reached its terminal velocity of -1750 km s^{-1}. The blue edge of the three profiles is variable, being at minimum displacement at Day 10 when the narrow DAC at its terminal velocity disappears

as strong. At the end of our campaign a new DAC seems to develop, which would set the recurrence timescale to be approximately 5 days. A Fourier analysis (cf. Paper II) of the 1992 dataset reveals a period of 5 days, but one has to take into account the relatively short time span covered by the data. We adopt a 5 days timescale characterizing the variability in 19 Cep, and assume that the 2.5 days encountered in 1991 is due to a weak intervening DAC such as observed for ξ Per and 68 Cyg.

The dip observed at -1750 km s^{-1} in the σ-ratio describing the variability of the Si iv line indicates that at this velocity the changes in absorption strength are relatively small. From the timeseries we see that at this position a DAC is continuously present. Therefore, a dip in the σ-ratio, if present, might be used as a diagnostic to measure the asymptotic velocity of DACs. The C iv edge is at minimum displacement at Day 5.6, and shifts towards higher velocity when the newly formed DAC accelerates through the Si iv profile. This underlines the difficulty in finding a one-to-one correlation between DAC behavior and edge variability, even for a given star.

4.9. *HD 210839 (λ Cep) O6 I(n)fp*

The observational history of this bright runaway Of star, originating from the parent Cep OB2 cluster with a radial velocity of -75 km s^{-1}(Gies & Bolton 1986), is well documented. Many observers have reported variability in the shape and strength of the emission features in the optical spectrum of λ Cep. In particular the double-peaked emission line of He ii at 4686 Å has been extensively studied for variability. Conti & Leep (1974) interpreted the changes in strength of the violet and red emission peak and the variable central absorption of this profile in terms of the revolution of an inhomogeneous wind around the star. This behavior was very well observed during our October 1989 campaign (see Henrichs 1991). The Hα emission line shows similar variability (Conti & Frost 1974; Ebbets 1982). Fullerton (1990) found dramatic *lpv* in optical He i and C iv lines. According to Henrichs (1991) the variations in the deep-photospheric He i line at 4713 Å are most likely caused by non-radial pulsations. The rapid rotation of λ Cep is indicated by the large value for $v \sin i$ (214 km s^{-1}).

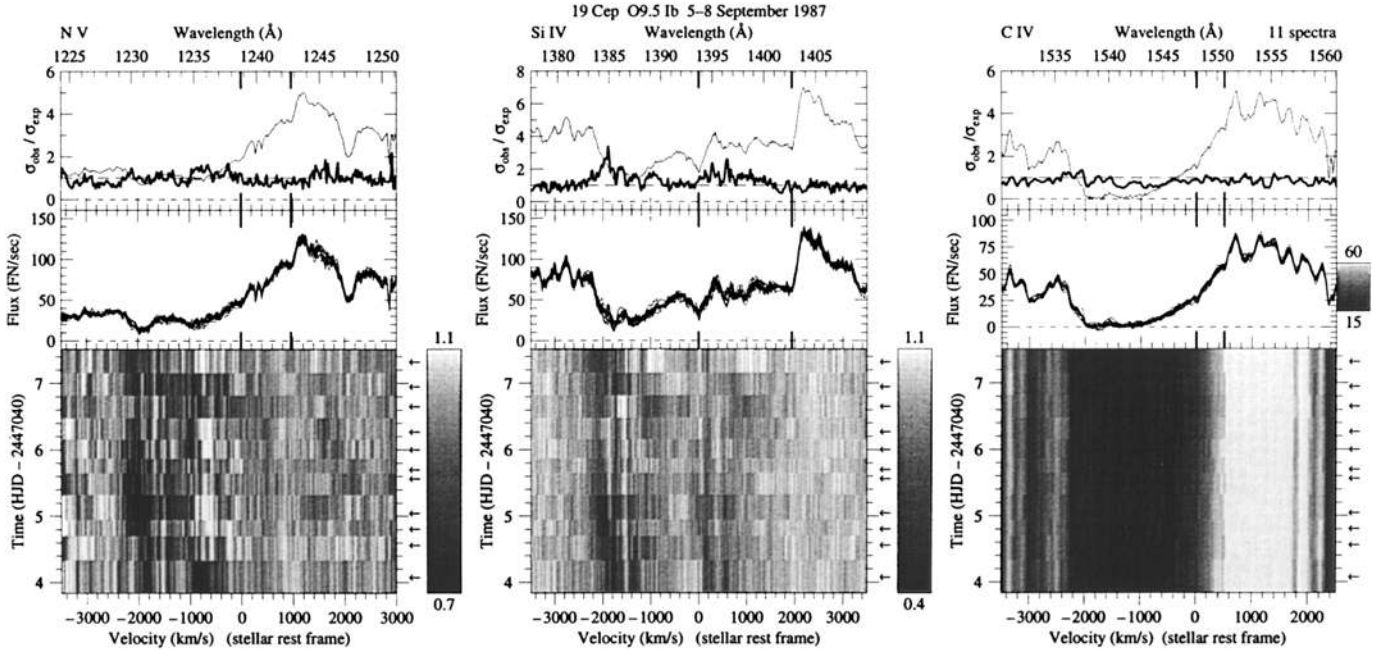

Fig. 16. As in Fig. 1: 19 Cep O9.5 Ib in September 1987. Given the long timescale of wind variability present in the previous dataset, the limited time span covered by these observations might explain the absence of a developing DAC. A weak DAC can be found at its asymptotic velocity

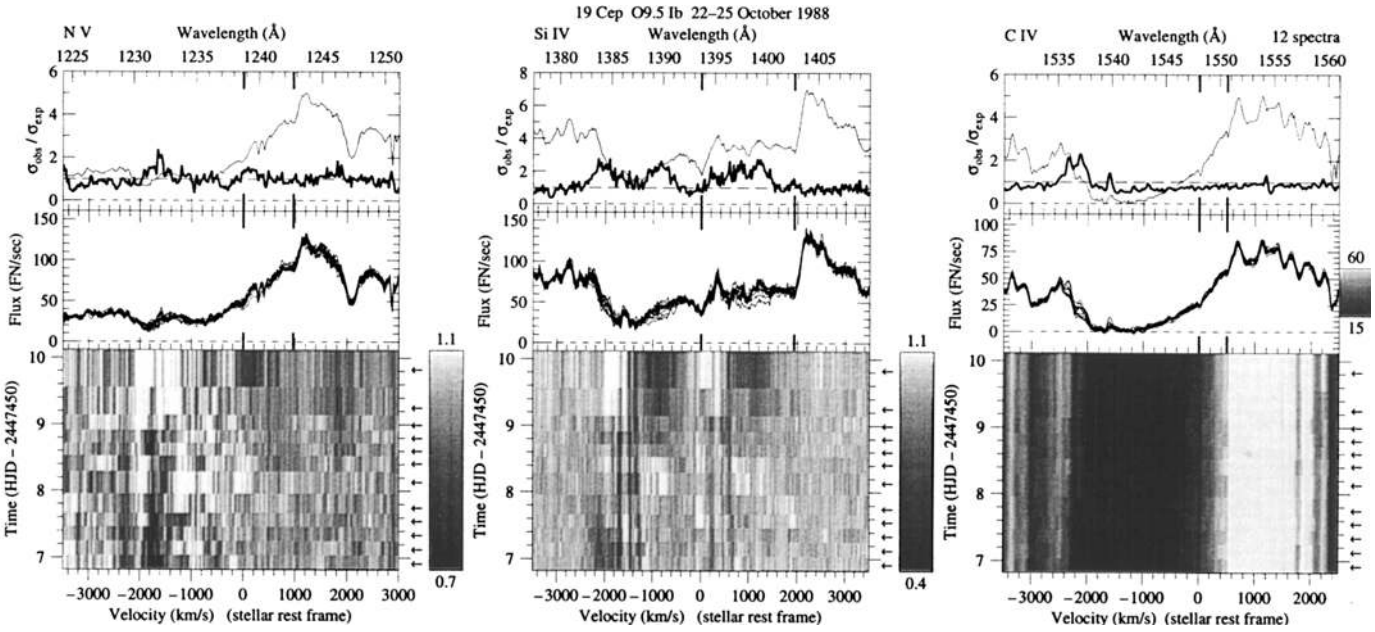

Fig. 17. As in Fig. 1: 19 Cep O9.5 Ib in October 1988. Also in this dataset the variations occurring in the unsaturated P Cygni lines are not very pronounced. Probably, a new DAC starts to develop at the end of the campaign

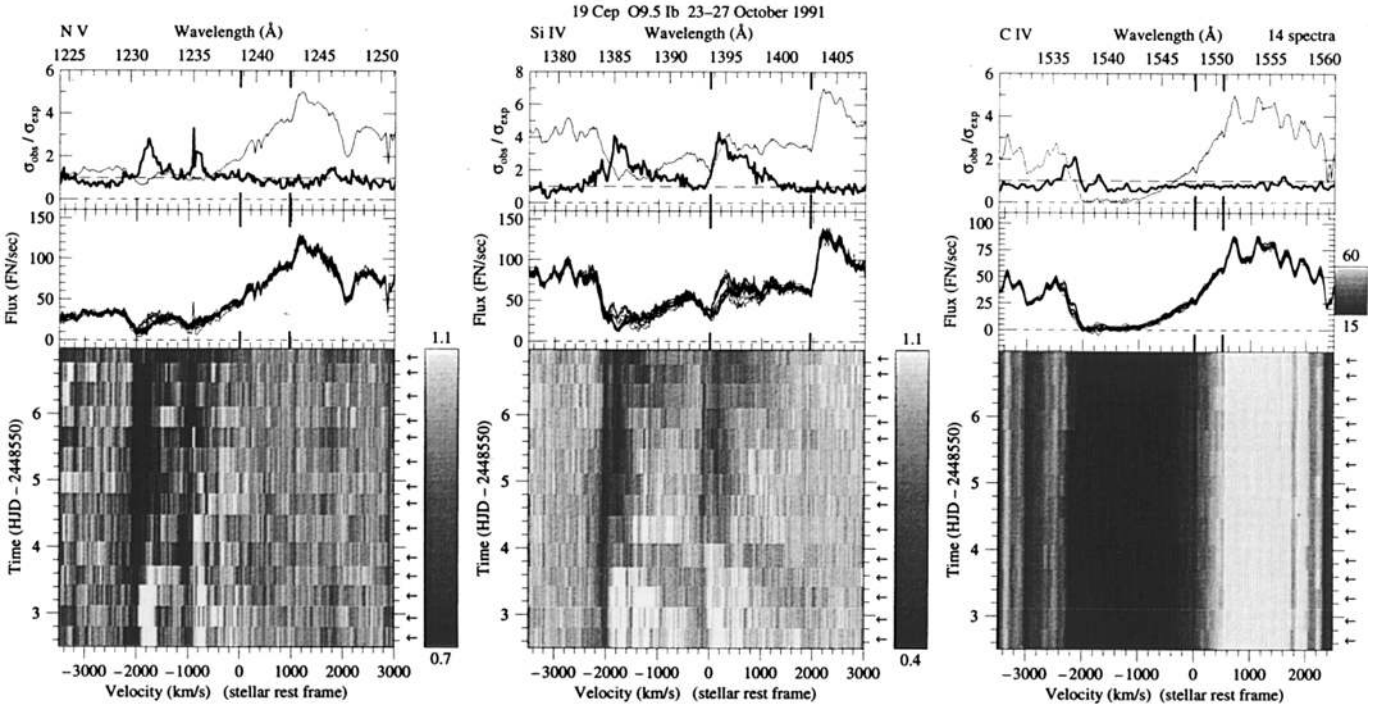

Fig. 18. As in Fig. 1: 19 Cep O9.5 Ib in October 1991. At Day 4 a DAC appears in the Si IV profile. Close to the end of our observations, around Day 6.5, we also note the presence of extra absorption at intermediate velocities, possibly the appearance of another DAC. This would mean that this year the DACs repeat on a time interval that is half of the 5-day timescale measured in November 1992 (Fig. 19)

HKZ reported for the first time the presence of DACs in the partly saturated Si IV doublet obtained in August 1986 (see Fig. 20), taking advantage of representing the spectra by means of grey-scale figures. Also the position of the blue edge of the strongly saturated UV resonance lines gradually changed with time (on a timescale of about 2 days) which strongly correlates with equivalent-width changes in the He II 4686 Å line at velocities below 400 km s^{-1} (Henrichs 1991). Fortunately, during the August 1986 campaign we obtained six IUE spectra within 1.5 days and were able to resolve the evolution of a DAC in time. The DAC accelerated within one day towards its terminal velocity at approximately −2000 km s^{-1}, derived from the nearly saturated red doublet component of the Si IV resonance lines. The σ-ratio does not indicate significant variations in the N V doublet, but shows a very pronounced edge variability in the Si IV and C IV lines, with maximum amplitude at −2300 and −2500 km s^{-1}, respectively. Around Days 5 and 8.5 the C IV edge is shifted towards its maximum position at −2500 km s^{-1}.

In the campaigns in September 1987 (Fig. 21) and October 1988 (Fig. 22) we obtained a dozen UV spectra which show the rapid evolution and reappearance of DACs, but the high saturation level of the profiles frustrates a detailed overview of their evolution. The red component of the Si IV resonance doublet shows that the variations extend from −600 to −1700 km s^{-1}, and the edge variability occurs at −2450 km s^{-1} in the C IV doublet. The emission peak of the C IV P Cygni profile has a triangular shape (as was the case for α Cam). In 1988 the σ-ratio has a peak in the N V profile, but this is due to one incorrectly calibrated spectrum, which shows up in the overplot in the middle panel of Fig. 22. The saturated part of the C IV profile is found to have a σ-ratio smaller than one: this is caused by the fact that the estimation of the expected variance at these low (i.e. zero) flux levels is based on the region around Lyman α where the flux calibration is uncertain (cf. Henrichs et al. 1994a), resulting in an overestimation of $\sigma_{\rm exp}$ at these flux levels. The October 1989 IUE observations were covered by optical observations (Henrichs et al. 1991); significant variations appear only in the edge of the Si IV and C IV profiles, on a timescale of about two days (Fig. 23). The Si IV profile appears to be saturated over a wider velocity range than observed in previous campaigns.

In 1991 we observed λ Cep twice; in February we monitored this star during 5 days and found dramatic changes in the blue edge of the Si IV and C IV lines (Fig. 24). Several DACs migrate through the Si IV profile; a remarkably strong component appears at Day 11 when a previous DAC (which developed at about Day 10) arrives at its asymptotic velocity of −2000 km s^{-1}. During this occasion the C IV edge shifts shortward more than 200 km s^{-1}. Although in October 1991 the amplitude of the

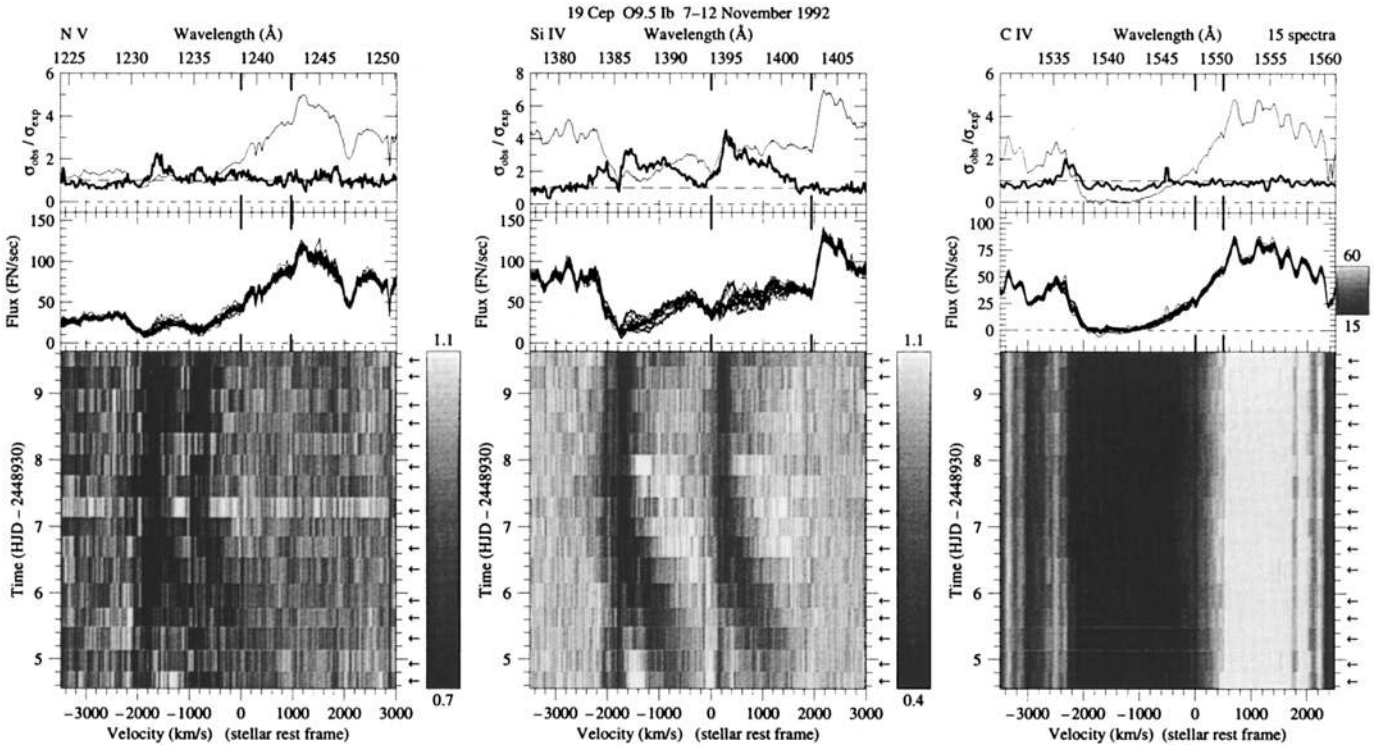

Fig. 19. As in Fig. 1: 19 Cep O9.5 Ib in November 1992. A strong DAC appears in this series of observations. At the end of the campaign a second DAC starts to develop. This sets the recurrence timescale to about 5 days for 19 Cep. The timeseries of 19 Cep provide strong support for our conclusion that slow stellar rotation is linked with a long characteristic timescale of variability and slow acceleration of DACs

variations is much smaller than observed in February 1991, the high time-resolution of this series enables the detection of four migrating DACs in the Si IV lines. From these observations (Fig. 25) we conclude that the recurrence timescale of DACs is about 1.4 days for λ Cep, which is again about equal to the time needed for a DAC to approach its terminal velocity. The edge of the saturated profiles (the edge of N V is partly obscured by the Lyman α interstellar absorption) is quite steady, showing an increase in velocity around Day 4.

4.10. *HD 214680 (10 Lac) O9 V*

This well-known main sequence star most-likely is a slow rotator ($v \sin i = 32$ km s^{-1}), although it might be that it is pole-on. It exhibits very subtle *lpv* in its optical spectrum (Smith 1977). Smith attributed this *lpv* to low order non-radial pulsations with a period of 4.9 hours, and classified 10 Lac as a 53 Per variable. The ultraviolet spectrum of 10 Lac contains only weak stellar-wind features, but LGS reported the presence of narrow absorption components in the O VI and N V resonance lines at about -900 km s^{-1}. PH did not detect any DACs in the unsaturated C IV profile. Although unsaturated, this profile has a remarkable shape, probably because of blending by the underlying photospheric spectrum (see Fig. 26). The N V doublet shows some blue-shifted absorption up to -800 km s^{-1} where the profile reaches the continuum.

During the November 1992 campaign the strongest manifestation of variability in the wind of 10 Lac is found in the N V resonance doublet. From -700 to -1000 km s^{-1} the σ-ratio shows a peak, with maximum amplitude at -900 km s^{-1}. In the timeseries of this line we note the development and subsequent acceleration of a DAC at Day 7, starting at a velocity of about -700 km s^{-1}. The corresponding DAC in the C IV line is also visible. The acceleration of the DAC ends at a velocity of approximately -1000 km s^{-1} in about three days. This is the first time that the evolution of a DAC has been observed in ultraviolet spectra of 10 Lac.

5. Characteristics of observed variability

In this section we summarize the characteristics of wind variability in our sample of 10 O stars which follow directly from the presented observations. In general we can conclude that the UV resonance lines of the O stars in this study show variability to some extent, except in cases when the saturation of the line prohibits detection. In unsaturated P Cygni lines the changes in blue-shifted absorption are mainly due to migrating discrete absorption components, which accelerate from low velocity towards

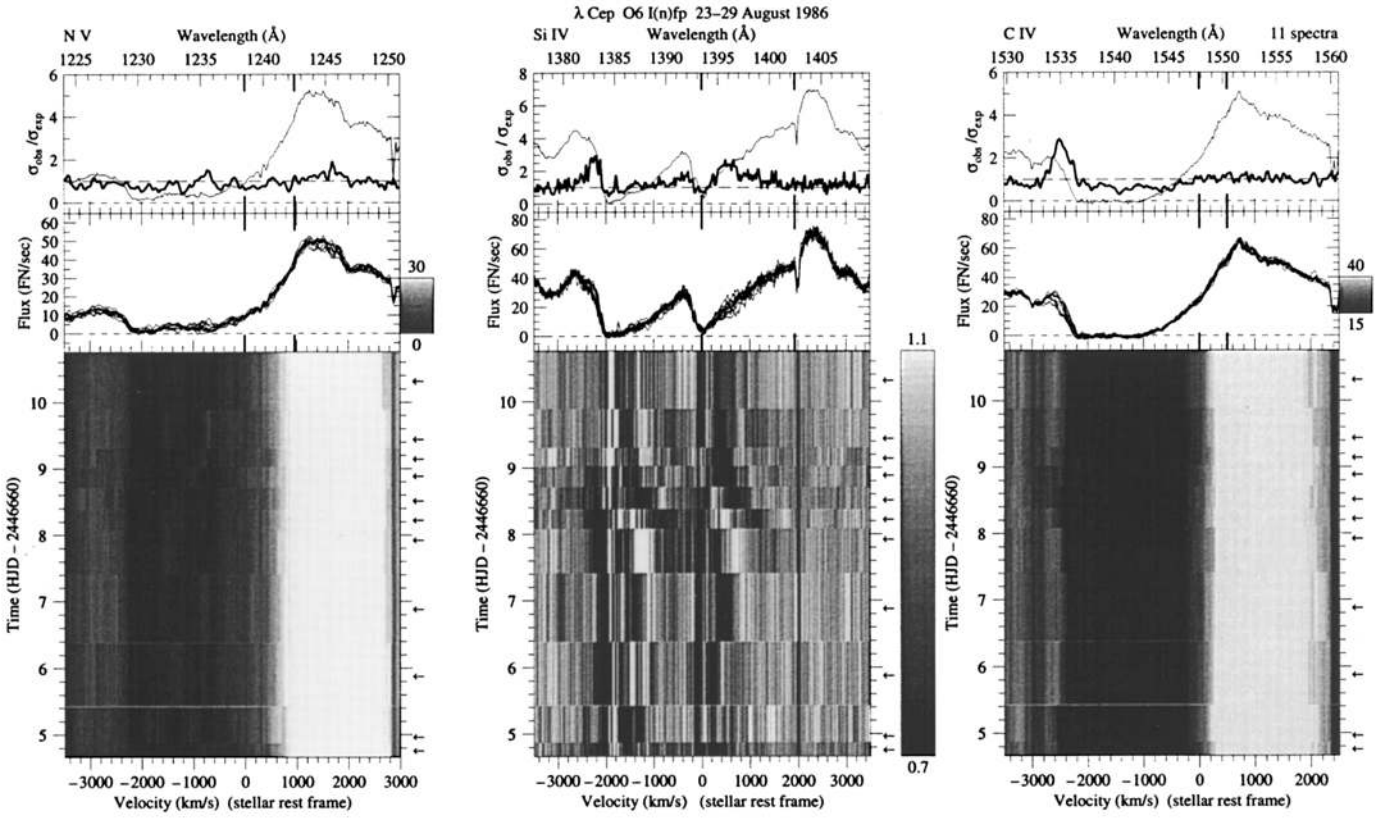

Fig. 20. As in Fig. 1: λ Cep O6 I(n)fp in August 1986. Only the top part of the grey-scale figure has sufficient time resolution (note the arrows at the right axis) to resolve the migration of a DAC in the Si IV doublet (displayed as quotient spectra). The DAC accelerates within one day towards its terminal velocity (approximately -2000 km s^{-1}, derived from the nearly saturated right doublet component of the Si IV resonance lines). The σ-ratio does not indicate significant variations in the N V doublet, but shows a very pronounced edge variability in the Si IV and C IV lines, with maximum amplitude at -2300 and -2500 km s^{-1}, respectively

the terminal velocity of the wind. In saturated lines the steep blue edge varies in all cases when DACs are found in other lines. Obviously, the amplitude of the variations is different from star to star, as is the observed timescale.

5.1. *Extent of variability*

In Table 4 we have listed the velocity range (in km s^{-1}) for which wind variability is observed in each individual star, based on the σ-ratio displayed in the top panel of the figures. Some stars (like ξ Per and HD 34656) vary over the full range of wind velocities, and the maximum amplitude is always found at a velocity larger than half the terminal velocity of the wind (see the σ-ratio displayed in the upper panels of the grey-scale figures). The highest velocity reached by DACs is also indicated in the table, if we were able to follow the evolution of a DAC during at least one of the observing campaigns. For 15 Mon and λ Ori we assumed that the central velocity of the persistent component is a good representation of the terminal velocity of the wind. Since the central velocity of the absorption components is one of the three parameters used to model the DACs (cf. Paper II), the highest velocity reached by DACs can be precisely determined. For 15 Mon and 10 Lac we did not detect any variability in the Si IV doublet, probably due to the photospheric nature of this line in main sequence stars (cf. Walborn & Panek 1984).

IUE observations of the O4 I(n)f star ζ Pup ($v \sin i =$ 230 km s^{-1}) were analysed by Prinja et al. (1992). Time series of the ultraviolet resonance lines revealed the wide range in velocity of wind variability in the Si IV ($\sim 750 -$ 2300 km s^{-1}) and C IV ($\sim$ 2600 $-$ 2900 km s^{-1}) doublets, and also the subordinate N IV line ($\sim$ 500 $-$ 1500 km s^{-1}). The latter line exhibits, just like the Si IV profile, the development and further evolution of DACs up to a maximum velocity of 2450 km s^{-1}. The observed recurrence time is about 15 hours. The saturated N V and C IV profiles show fluctuations in blue-edge velocities up to 200 km s^{-1}. The rapidly rotating ($v \sin i =$ 400 km s^{-1}) and non-radially pulsating O9.5 V star ζ Oph has been studied by Howarth et al. (1993). For this star the observed range of variability is very limited ($\sim$ 1200 $-$ 1600

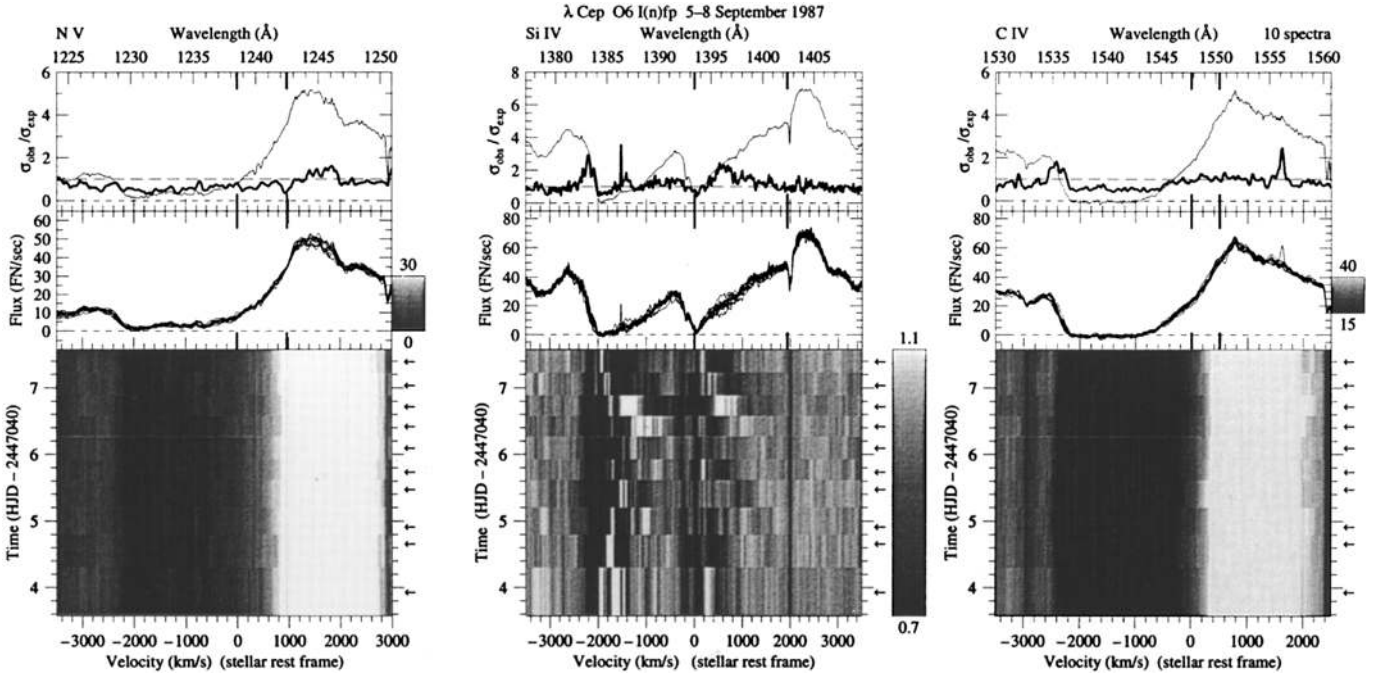

Fig. 21. As in Fig. 1: λ Cep O6 I(n)fp in September 1987. We cannot resolve the rapid evolution of DACs in this timeseries because of insufficient time resolution. Note the triangular shape of the P Cygni emission in the C IV doublet

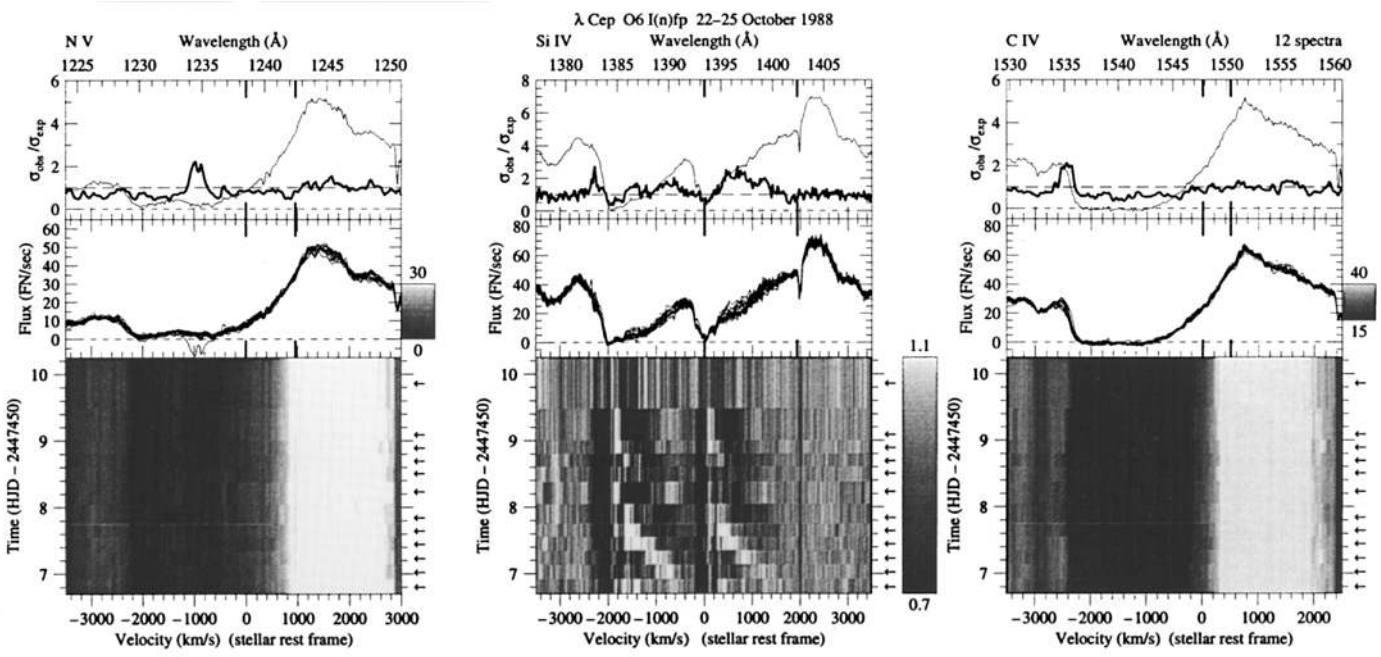

Fig. 22. As in Fig. 1: λ Cep O6 I(n)fp in October 1988. Several DACs migrate through the Si IV profile. The σ-ratio has a peak in the N V profile, but this is due to one wrongly calibrated spectrum, which shows up in the overplot in the middle panel. The saturated part of the C IV profile is found to have a σ-ratio smaller than one: this is caused by the fact that the estimated $\sigma_{\rm exp}$ at these low (i.e. zero) flux levels is based on the region around Lyman α where flux calibration is uncertain (cf. Henrichs et al. 1994a), resulting in an overestimation of $\sigma_{\rm exp}$ at these flux levels

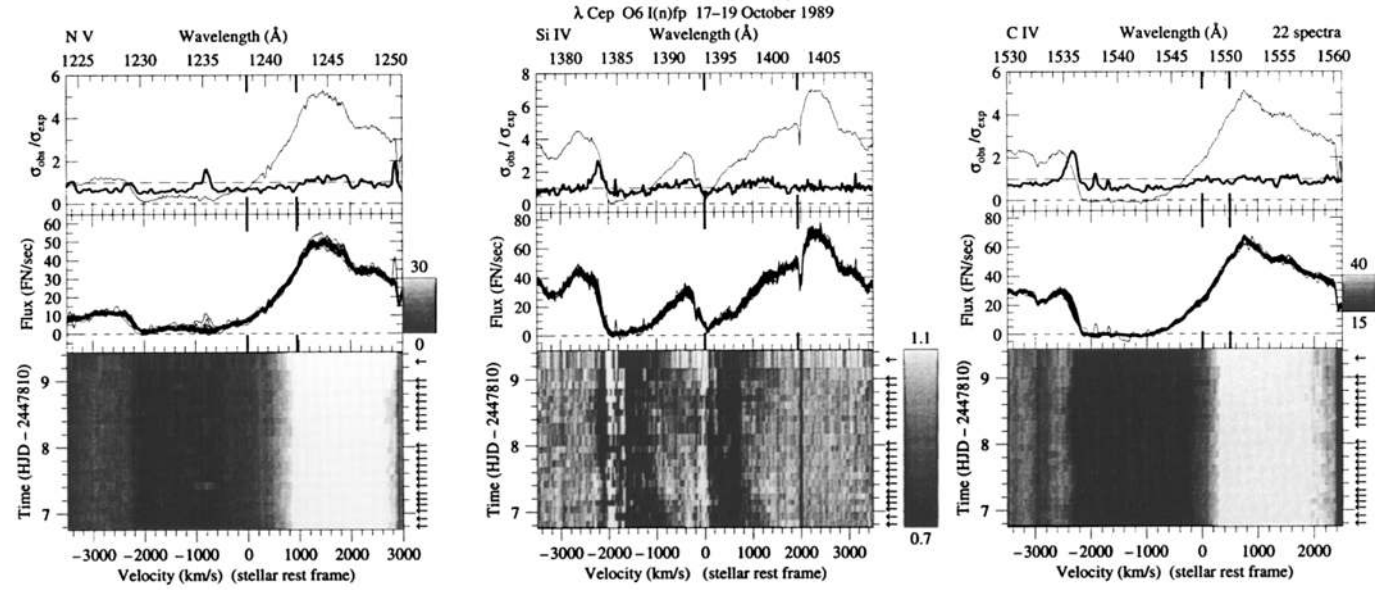

Fig. 23. As in Fig. 1: λ Cep O6 I(n)fp in October 1989. The C IV and Si IV profile show a significant change in the blue edge on a timescale of about two days. The Si IV profile seems to be saturated over a wider range in velocity than observed in previous years. Simultaneous optical spectroscopy (Henrichs et al. 1991) revealed that the He II 4686 Å line varies in concert with the C IV and N V blue edge. The deep-photospheric He I 4713 Å line exhibits *lpv* that might be attributed to non-radial pulsations

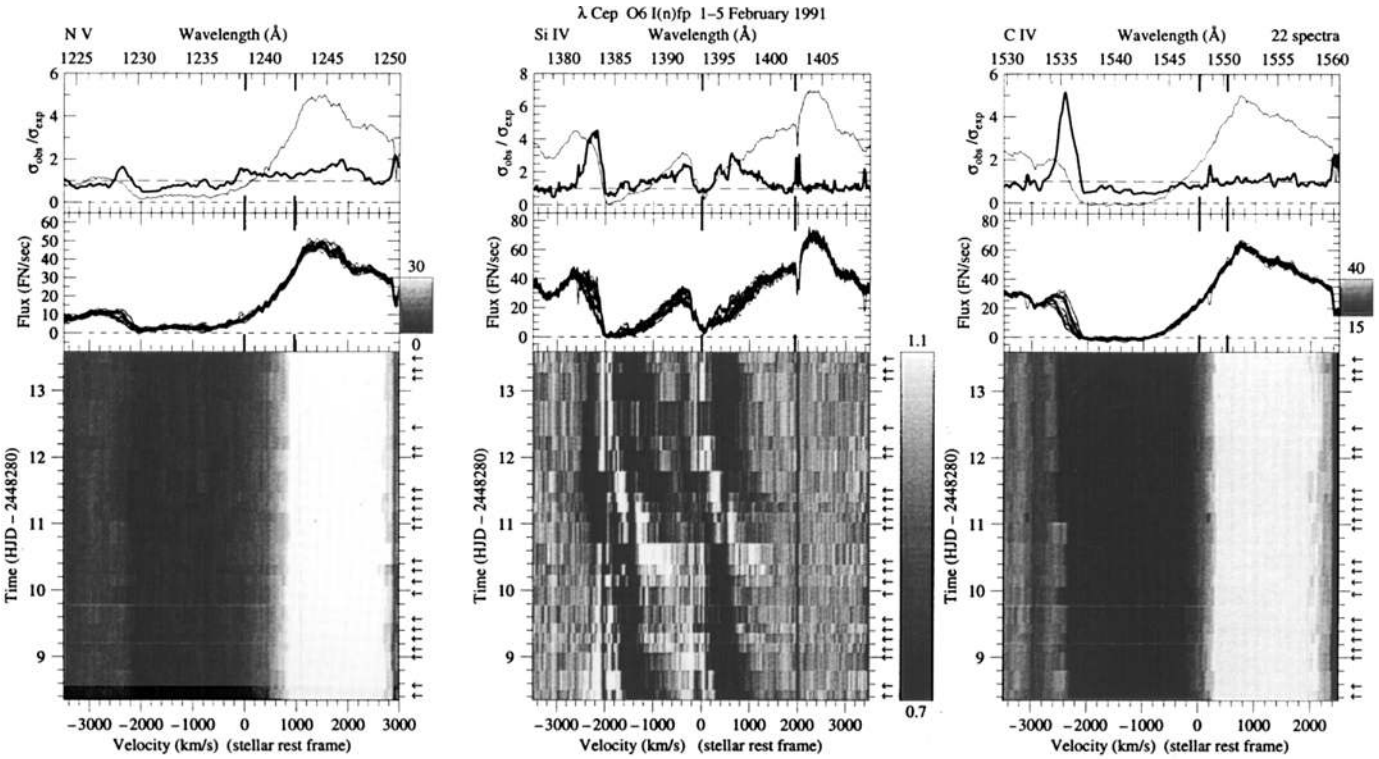

Fig. 24. As in Fig. 1: λ Cep O6 I(n)fp in February 1991. Several DACs migrate through the Si IV profile. A strong DAC appears in the Si IV line at Day 11 while an evolved component (which appeared at Day 10) arrives at its asymptotic velocity of -2000 km s^{-1}. During this occasion the C IV edge shifts more than 200 km s^{-1} towards the blue. The amplitude of the edge variability in this dataset is the largest we encountered for λ Cep

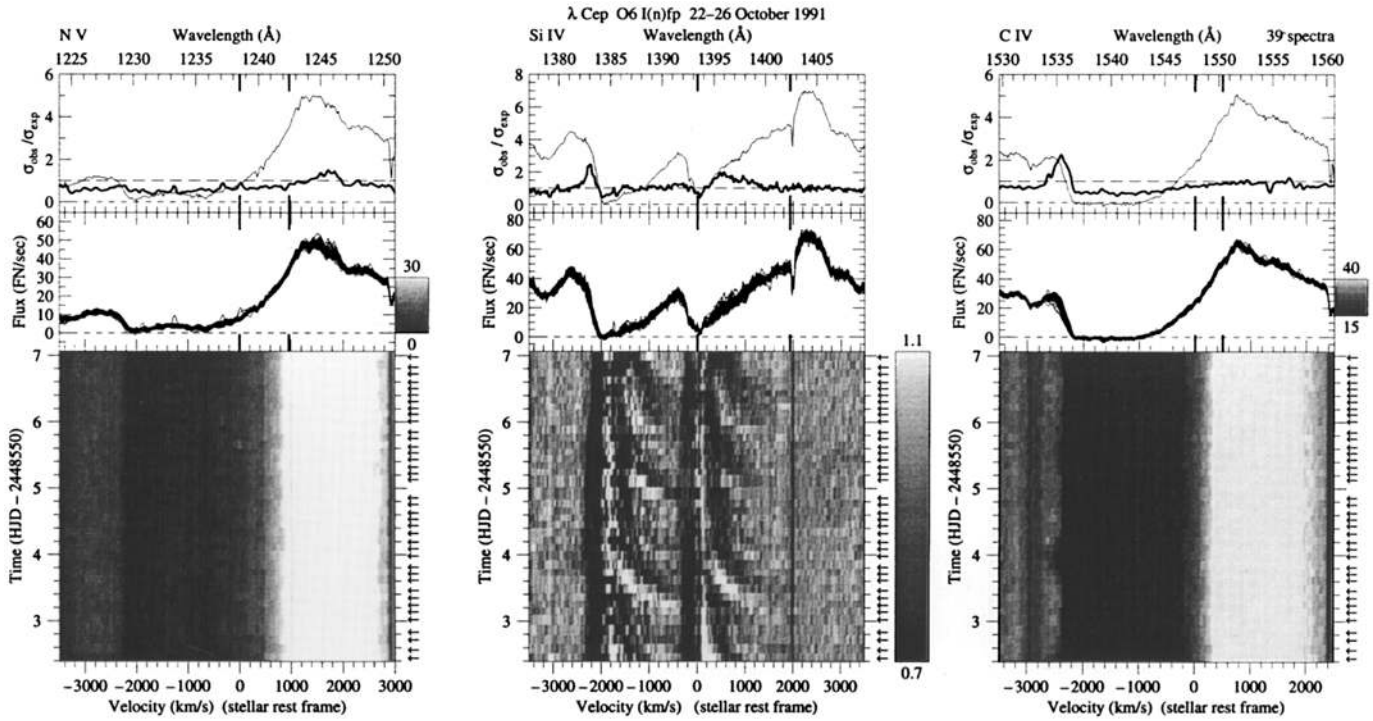

Fig. 25. As in Fig. 1: λ Cep O6 I(n)fp in October 1991. Four DAC events can be distinguished in the partly saturated Si IV doublet. From this dataset we find a DAC recurrence timescale of about 1.4 days

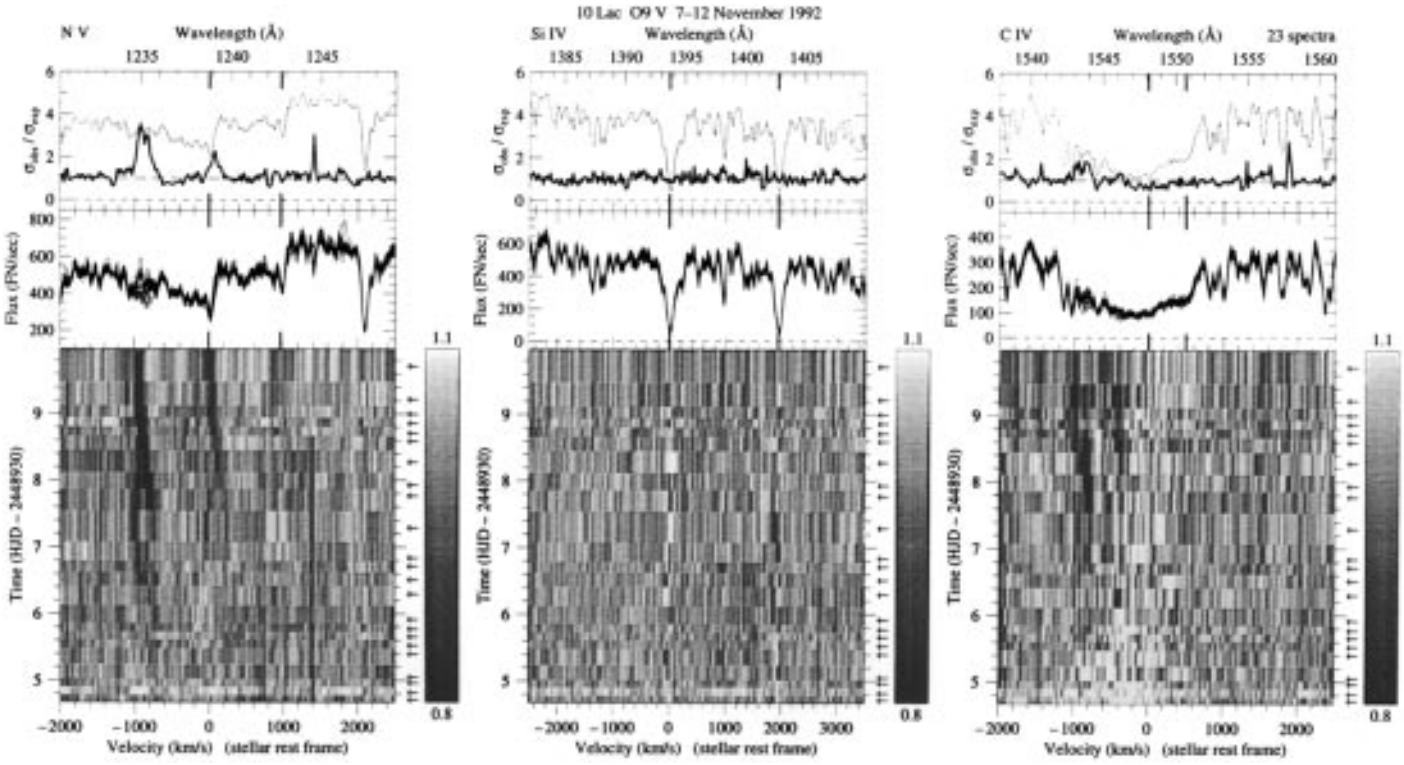

Fig. 26. As in Fig. 1: 10 Lac O9 V in November 1992. The appearance of a slowly migrating DAC can be noticed in both the N V and the C IV resonance lines. The Si IV line has a photospheric origin and does not show any wind variability

Table 4. The extent of wind variability (in km s^{-1}, the given values represent negative velocities) in the sample of O stars as derived from the σ-ratio. Listed are the range of variability in the subordinate N IV line (for ξ Per only) and the N V, Si IV, and C IV resonance lines. The maximum value measured for the σ-ratio ($\sigma^{\max}$) indicates the amplitude of variability. The maximum velocity reached by DACs (if present) is tabulated in the last column. For detailed information about DAC parameters we refer to Kaper et al. (1995b, Paper II)

Star	N IV	$\sigma^{\max}$	Si IV	$\sigma^{\max}$	N V	$\sigma^{\max}$	C IV	$\sigma^{\max}$	$v^{\max}_{\rm DACs}$
ξ Per	200-700	1.5	0-2500	7	300-2700	3	2400-2700	3	2250
α Cam			1800-1950	2					
HD 34656			200-2400	4.5	1400-2000	2.5	2200-2600	3.5	1850
λ Ori A			1800-2100	2.5	(300-2300)	3.5	(1800-1900)	2	2000
ζ Ori A			700-2300	3	700-2100	2	1800-2300	2	1700
15 Mon					400-2500	2.5	2100-2400	1.5	1950
68 Cyg			800-2600	5	800-2700	4	2400-2800	4	2350
19 Cep			500-2300	6	1000-2200	5	2000-2400	2.5	1750
λ Cep			600-1700	4	2100-2300	2	2100-2600	5	(2000)
10 Lac					700-1000	3	700-1000	2	1000

km s^{-1} in the N V and C IV resonance lines), although the blueward migration of DACs is very pronounced. The recurrence timescale of the phenomenon is $\sim$ 20 hours and the asymptotic velocity reached by DACs is 1480 km s^{-1}.

5.2. *DAC behavior and edge variability*

For 7 out of 10 O stars we could identify the evolution of DACs in one or more timeseries. For λ Ori and 15 Mon a persistent absorption component is visible in the spectra at a constant velocity of -2000 km s^{-1}, which we interpreted as the terminal velocity reached by DACs. The strongly saturated P Cygni profiles of α Cam prohibited the detection of any DAC (if present). All detected DACs move from low to high velocity on a timescale comparable to the characteristic timescale of variability (see next subsection), which means that DACs in the wind of stars with *higher* $v \sin i$ accelerate *faster* towards their terminal velocity. For some stars (ξ Per and 68 Cyg) the velocity reached by DACs differs from event to event: for ξ Per this difference is about 350 km s^{-1}.

Although the characteristic variability and acceleration timescales remain the same over many years, we note that the strength of the DACs is not constant (e.g. 19 Cep) and differs from event to event. The width of a DAC becomes smaller when its central velocity increases. This is similar to what has been found for other well-studied cases (e.g. Prinja et al. (1987) in the case of ξ Per and Prinja & Howarth (1988) in the case of 68 Cyg).

The position of the steep blue edge in the ultraviolet P Cygni profiles changes gradually with time, showing shifts in velocity on a 10% level. In some timeseries the edge shifts to a minimum in velocity when a DAC (visible in an unsaturated P Cygni line) at its terminal velocity disappears (e.g. 19 Cep). The edge sometimes shifts towards higher velocity when a newly formed DAC approaches its terminal velocity. The amount of change in position of the blue edge could depend on the strength of the DACs. The search for a possible relation between DAC behavior and edge variability is hampered by the fact that several DACs can be present in the P Cygni profiles simultaneously. Close inspection of the variations in the presented timeseries suggests, however, that edge variability and DACs reflect the same phenomenon. The morphology of these changes depends on the optical depth of the underlying P Cygni profile of the considered line. If the optical depth is small, the profile is unsaturated and one observes DACs (and sometimes also edge variability, see e.g. ξ Per and 19 Cep) migrating through the profile. If the optical depth is sufficiently large, the profile is saturated, obscuring any changes in column density. At velocities which exceed the terminal velocity of the wind (which is identified as $v_{\rm black}$ by Prinja et al. 1990) the profile is not saturated and therefore will show similar variability as in the edge of the unsaturated lines (see also Fig. 7 in Henrichs et al. 1994a).

Although in many cases variations at the edge velocity can be linked to the evolution of a particular DAC in an unsaturated profile, it might be that different phenomena with different timescales are playing a role. From the currently available observations it is not clear whether one could derive if the observed complexity has one unique interpretation.

5.3. *Characteristic timescale of variability*

In Table 5 we compare the observed characteristic timescale of DAC variability $t_{\rm DAC}$ with the expected rotation period of the star. An upper and a lower limit for the rotation period of the star can be calculated from the observed $v \sin i$ and the critical rotation velocity $v_{\rm crit}$, respectively. The values for the stellar radius are taken from

Table 5. The characteristic timescale of DAC variability is listed for each target. These results are consistent with the values obtained after detailed modeling of the DACs (Paper II). $t_{\rm DAC}$ is compared to the minimum and maximum rotation period, estimated from the stellar parameters given in Table 1. The escape velocities, needed to calculate the critical velocities, are corrected for the radiative force on electrons (from Howarth & Prinja 1989). The stars are ordered by $P_{\rm max}$

Name	$v_{\rm esc}$ (km s^{-1})	$v_{\rm crit}$ (km s^{-1})	$P_{\rm min}$ (days)	$v \sin i$ (km s^{-1})	$P_{\rm max}$ (days)	$t_{\rm DAC}$ (days)
68 Cyg	910	631	1.1	274	2.6	1.3
ξ Per	980	711	0.8	200	2.8	2.0
λ Cep	990	709	1.2	214	4.0	1.4
HD 34656	1040	726	0.7	106	4.8	0.9
15 Mon	1120	785	0.6	63	8.1	> 4.5
λ Ori A	910	654	0.9	53	11.5	> 5
19 Cep	720	511	1.8	75	12.2	~ 5
α Cam	680	483	2.3	85	13.2	
ζ Ori A	630	451	3.3	110	13.4	~ 6
10 Lac	1110	757	0.6	32	14.3	> 5

Table 1 and the escape velocities, corrected for electron scattering, were obtained from HP. For some stars (ξ Per, 68 Cyg, and 19 Cep) we had to redefine the characteristic timescale of variability by the time interval between two successive *strong* DACs, to account for some weak DACs that sometimes appear in between these strong events. In these cases the recurrence timescale cannot be derived unambiguously. This alternative definition for $t_{\rm DAC}$ better represents the observed regular repetition of a characteristic DAC "pattern".

If $t_{\rm DAC}$ reflects the corotation of matter around the star, $t_{\rm DAC}$ should be a direct measure of the stellar rotation period. The stars with low $v \sin i$ show a relatively long recurrence (and acceleration, see above) timescale for the DACs. On the other hand, stars with high $v \sin i$ value show a rapid recurrence of DACs, including the rapid rotators ζ Pup (Prinja et al. 1992) and ζ Oph (Howarth et al. 1993). The characteristic timescale of variability never exceeds the maximum rotation period as indicated in Table 5. From this, and the fact that the "pattern" of variability is constant over many years, we conclude that stellar rotation plays a crucial role in the observed development and dynamical evolution of DACs. The evidence presented here considerably substantiates the earlier similar suggestion independently made by Prinja (1988) and HKZ.

5.4. *Subordinate lines*

For ξ Per we detected significant variations in blue-shifted absorption in the subordinate N IV line at 1718 Å. These variations are directly related to the DACs present in the Si IV line, but occur at lower velocity. Prinja et al. (1992) detected variability at low velocitiy in the N IV profile of the O4 I(n)f star ζ Pup, with the difference that they could resolve the blueward migration of DACs such as observed in the Si IV line. Since subordinate lines arise from excited levels, the N IV ions producing the 1718 Å line are not in the ground state (in contrast to the resonance lines). Therefore, the 1718 Å line of N IV is only formed in a relatively dense part of the (expanding) atmosphere. Hence, we consider these low-velocity variations in the subordinate N IV line as evidence that wind variability originates close to the stellar surface. In Paper II we will show that low-velocity variations are also found in subordinate lines of three other O stars in this study (HD 34656, 68 Cyg, and λ Cep).

6. Conclusions and discussion

The most obvious conclusions from the quantified results presented are the strong confirmation of the ubiquitous variability of winds of O stars, and the critical correlation between rotation of the star and the behavior of DACs.

Several suggestions have been put forward to explain the variability of stellar winds: corotating interacting regions such as applied to the solar wind case (Mullan 1984), magnetic loops releasing matter just above the stellar surface (Underhill & Fahey 1984), or the episodic ejection of a high-density shell (Lamers et al. 1978; Henrichs et al. 1983). Prinja & Howarth (1988) argued on grounds of a self-consistent phenomenological model describing the observed opacity depth enhancements in the line of sight that DACs do not propagate from the photosphere. Howarth (1992) further questioned their possible photospheric origin based on the absence of infrared emission at 10 μm during the appearance of a DAC in the UV resonance lines of the O7.5 giant 68 Cyg; this IR emission should be observed if the shell model is correct.

A very promising ingredient was added to the discussion (e.g. Owocki et al. 1988; Feldmeier 1995) by showing that the unstable character of the acceleration mech-

anism in a radiation-driven wind can result in a highly structured and variable flow. The time evolution of such a clumpy wind can in principle explain the variable P Cygni profiles (Puls et al. 1993), but the observed slow acceleration of DACs (e.g. Prinja & Howarth 1988) and their recurrence timescales are not consistent with the clumpy wind model. Calculations show (cf. Owocki 1992) that the inclusion of scattering suppresses the line instability at the base of the flow, resulting in a structured wind only from a few stellar radii above the stellar surface to further out in the wind, possibly explaining why the largest amplitude of variability is found at velocities exceeding 0.5 v_∞. Waldron et al. (1993) note, however, that the IR emission as predicted by the Owocki model calculations is also not consistent with observations, and obviously much is still to be done. We stress that in all calculations the stellar rotation has not been taken into account, because of the very high degree of complexity.

More recently it is getting clear that a distinction should be made between relatively small-scale, stochastic variability and variations due to large-scale structures in the stellar wind (Owocki 1994; Kaper & Henrichs 1994; Henrichs et al. 1994b). The former type of variability might be related to the strong intrinsic instability of the radiation-driven flow which leads to small-scale structure in the wind, causing the observed saturation of UV P Cygni profiles and X-ray flux. The latter variations might reflect co-rotating structure in the wind induced by wind-flow properties that depend on the boundary conditions set at the base of the stellar wind. When such a structure obscures a significant part of the stellar photosphere, a DAC would be observed in the UV resonance lines. We defer a further discussion of the DACs to Paper II, which contains the quantitative results of model fits of DACs.

Acknowledgements. The authors wish to thank the IUE Observatory staff at both NASA and VILSPA for their dedicated efforts in executing this difficult program. We also thank the referee Alex Fullerton who provided us with useful comments that helped to improve the paper. LK acknowledges the support of the Netherlands Organization for Scientific Research (NWO) under grant 782-371-037. Part of this work was supported by NASA grant NAS5-32473.

A. Log of observations

Tables listing the Logs of IUE Observations described in this paper are only available in electronic form at the CDS via anonymous ftp 130.79.128.5. The table number corresponds to the figure number in the paper. The involved O star and the observing period are mentioned in the table header. Column 1 gives the sequence number; Column 2 lists the identification number of the observation obtained with the Short Wavelength Prime camera on IUE; Column 3 gives the day of the month; Column 4 provides the start time of the observation (UT); Column 5 lists the exposure time (in min:sec); Column 6 gives the Julian Day at mid-exposure. As an example we list the first five lines of Table A1:

Table A1. ξ Per, September 1987

#	SWP	Date	Start h:m (UT)	$t_{\rm exp}$ m:s	JD −2447040
1	31716	5	8:26	1:10	3.852
2	31719		11:19	1:20	3.972
3	31721		13:02	1:15	4.044
4	31726		23:39	1:15	4.486
5	31728	6	0:56	1:15	4.540

References

Alduseva V.Ya., Aslanov A.A., Kolotilov E.A., Cherepashchuk A.M., 1982, Sov. Astr. Lett. 8, 386
Barker P.K., 1984, AJ 89, 899
Barlow M.J., 1979, in IAU Symp. 83, Mass Loss and Evolution of the O-type Stars. In: Conti P.S., de Loore C.W.H. (eds.), p. 119
Berghöfer T.W., Schmitt J.H.M.M., 1994, Sci 265, 1689
Bianchi L., Bohlin R., 1984, A&A 134, 31
Blaauw, A., 1992, in Proc. Massive Stars: Their Lives in The Interstellar Medium. In: Cassinelli, Churchwell (eds.), ASP Conf. Ser. 35, p. 207
Castor J.I., Abbott D.C., Klein R.K., 1975, ApJ 195, 157
Conti P.S., 1974, ApJ 187, 539
Conti P.S., Frost S.A., 1974, ApJ 190, L137
Conti P.S., Leep E.M., 1974, ApJ 193, 113
Conti P.S., Ebbets D., 1977, ApJ 213, 438
De Vries C.P., 1985, A&A 150, L15
Ebbets D., 1980, ApJ 235, 97
Ebbets D., 1982, ApJS 48, 399
Feldmeier A., 1995, A&A 299, 523
Fullerton A.W., 1990, Thesis, University of Toronto
Fullerton A.W., Gies D.R., Bolton C.T., 1991a, ApJ 368, L35
Fullerton A.W., Bolton C.T., Garmany C.D., et al., 1991b, ESO Workshop on Rapid variability of OB stars: Nature and diagnostic value. In: Baade D. (ed.), p. 213
Garmany C.D., Conti P.S., Massey P., 1980, ApJ 242, 1063
Gathier R., Lamers H.J.G.L.M., Snow T.P., 1981,
Gehrz R.D., Hackwell J.A., Jones T.W., 1974, ApJ 191, 675
Giddings J.R., 1983, ESA IUE Newslett. 17, 53
Giddings J., 1983a, IUE Newslett. 12, 22
Giddings J., 1983b, SERC Starlink User Note 37
Gies D.R., 1987, ApJS 64, 545
Gies D.R., Bolton C.T., 1986, ApJS 61, 419
Gies D.R., Mason B.D., Hartkopf W.I., et al., 1993, AJ 106, 2072
Grady C.A., Snow T.P., Cash W.C., 1984, ApJ 283, 218
Hayes D.P., 1984, AJ 89, 1219
Henrichs H.F., 1984, Proc. 4th Europ. IUE Conf., ESA SP-218, p. 43
Henrichs H.F., 1988, NASA/CNRS "O, Of and Wolf-Rayet Stars". In: Conti & Underhill (eds.), p. 199

Henrichs H.F., 1991, ESO Workshop on Rapid variability of OB stars: Nature and diagnostic value. In: Baade D., p. 199
Henrichs H.F., Hammerschlag-Hensberge G., Howarth I.D., Barr P., 1983, ApJ 268, 807
Henrichs H.F., Kaper L., Zwarthoed G.A.A., 1988, in A Decade of UV Astronomy with the IUE Satellite (ESA SP-281), Vol. 2, p. 145 (HKZ)
Henrichs H.F., Gies D.R., Kaper L., et al., 1990, in Proc. Evolution in Astrophysics: IUE Astronomy in the era of new space missions, ESA SP-310, p. 401
Henrichs H.F., Kaper L., Ando H., et al., 1994, in Proc. Frontiers of Space and Ground-based Astronomy. In: Wamsteker W., Longair M.S., and Kondo Y. (eds.), Astroph. Space Sc. Lib. Kluwer, Dordrecht, p. 567
Henrichs H.F., Kaper L., Nichols J., 1994, A&A 285, 565
Henrichs H.F., Kaper L., Nichols J., 1994, in Proc. IAU Symp. 162 on Pulsation, Rotation and Mass Loss in Early-Type Stars. In: Balona, Henrichs, Le Contel (eds.), p. 517
Hoffleit D., Jaschek C., 1982, The Bright Star Catalogue (4th ed.), New Haven: Yale University Observatory
Howarth I.D., 1992, in Proc. "Nonisotropic and Variable Outflows from Stars", ASP Conf. Ser. 22. In: Drissen L., Leitherer C., Nota A. (eds.), p. 155
Howarth I.D., Prinja R., 1989, ApJ 69, 527 (HP)
Howarth I.D., Bolton C.T., Crowe R.A., et al., 1993, ApJ 417, 338
Howarth I.D., Smith K.C., 1995, ApJ 439, 431
Humphreys R., 1978, ApJS 38, 309
Jarad M.M., Hilditch R.W., Skillen I., 1989, MNRAS 238, 1085
Kaper L., 1993, Ph.D. thesis Univ. of Amsterdam
Kaper L., Henrichs H.F., Zwarthoed G.A.A., Nichols-Bohlin J., 1990, in Proc. NATO Workshop on Mass Loss and Angular Momentum of Hot Stars. In: Willson L.A., Bowen G., Stalio R., p. 213
Kaper L., Henrichs H.F., Nichols-Bohlin J., 1992, in Proc. Variable Stars and Galaxies. In: Warner B., ASP Conf. Ser. Vol. 30, p. 135
Kaper L., Henrichs H.F., 1994, in Proc. Instability and Variability of Hot-Star Winds. In: Moffat A., Owocki S., Fullerton A., St-Louis N., Ap&SS 221, 115
Kaper L., Henrichs H.F., Ando H., et al., 1995a (submitted to A&A)
Kaper L., Henrichs H.F., Nichols J., 1995b (Paper II) (in preparation)
Lamers H.J.G.J.M., Snow T.P., 1978
Lamers H.J.G.J.M., Gathier R., Snow T.P., 1982, ApJ 258, 186 (LGS)
Lamers H.J.G.J.M., Snow T.P., De Jager C., Langerwerf A., 1988, ApJ 325, 342
Lamers H.J.G.L.M., Leitherer C., 1993, ApJ 412, 771
Lupie O.L., Nordsieck K.H., 1987, 92, 214
Morton D.C., 1976, ApJ 203, 386
Mullan D.J., 1984, ApJ 283, 303
Musaev F.A., Snezhko L.I., 1988, Sov. Astr. Lett. 14, 68
Owocki S.P., 1992, in The Atmospheres of Early-Type Stars. In: Heber U., Jeffery C.S. (eds.). Springer: Berlin, p. 393
Owocki S.P., 1994, in Proc. Instability and Variability of Hot-Star Winds. In: Moffat A., Owocki S., Fullerton A., St-Louis N., Ap&SS 221, 3
Owocki S.P., Castor J.I., Rybicki G.B., 1988, ApJ 335, 914
Prinja R.K., 1988, MNRAS 231, 21P
Prinja R.K., Howarth I.D., 1986, ApJS 61, 357 (PH)
Prinja R.K., Howarth I.D., Henrichs H.F., 1987, ApJ 317, 389
Prinja R.K., Howarth I.D., 1988, MNRAS 233, 123
Prinja R.K., Barlow M.J., Howarth I.D., 1990, ApJ 361, 607
Prinja R.K., Balona L.A., Bolton C.T., et al., 1992, ApJ 390, 266
Puls J., Owocki S.P., Fullerton A.W., 1993, A&A 279, 457
Smith M.A., 1977, ApJ 215, 574
Snow T.P., 1977, ApJ 217, 760
Snow T.P., 1982, ApJ 253, L39
Snow T.P., Cash W., Grady C.A., 1981, ApJ 244, L19
Snow T.P., Jenkins E.B., 1977, ApJS 33, 269
Snow T.P., Morton D.C., 1976, ApJS 32, 429
Underhill A.B., 1975, ApJ 199, 691
Underhill A.B., Fahey R., 1984, ApJ 280, 712
Walborn N.R., 1972, AJ 77, 312
Walborn N.R., 1973, AJ 78, 1067
Walborn N.R., Panek R.J., 1984, ApJ 280, 712
Waldron W.L., Klein L., Altner B., 1994, ApJ 426, 725